CHARLES UNIVERSITY IN PRAGUE, FACULTY OF SCIENCE

Institute of Hydrogeology, Engineering Geology and Applied Geophysics

Contribution to the tectonic interpretation of the seismicity pattern of the Banda Arc, Southeast Asia

Příspěvek k tektonické interpretaci rozložení seismické aktivity
v ostrovním oblouku Banda, jihovýchodní Asie

DIPLOMA THESIS

Radka Matějková

Supervisor: **RNDr. Aleš Špičák, CSc.**
Advisers: **RNDr. Václav Hanuš, DrSc.**
RNDr. Jiří Vaněk, DrSc.

Prague, September 2008

Abstract

Contribution to the tectonic interpretation of the seismicity pattern of the Banda Arc, Southeast Asia

Tectonic structure of the Banda Arc in Southeast Asia is regarded as an extremely complicated unit as it is situated at the intersection of four lithospheric plates: Eurasian, Indo-Australian, Pacific, and Philippine. The present-day tectonic regime is arc-continent collision. The seismotectonic pattern of the Banda Arc region was studied using global seismological data. Relocated EHB hypocentral determinations for the period 1964 – 2004 and fault plane solutions of Harvard CMT data for the period 1976 – 2004 have been used. The analysis of spatial distribution of earthquake foci and the analysis of focal mechanisms enabled to distinguish the foci belonging to the Wadati-Benioff zone of the subducting plate from those occurring in the overriding plate. The analysis discriminated two opposite dipping subduction zones – southern Banda subduction and northern Seram subduction. The following specific phenomena were observed in the Wadati-Benioff zone: (i) unusual lateral bent of the Wadati-Benioff zone of the southern Banda subduction, (ii) intermediate-depth (100 – 220 km), vertically situated domain of the highest seismicity within the Wadati-Benioff zone of the southern Banda subduction, (iii) segment of shallow seismicity with uniform reverse focal mechanisms within the Wadati-Benioff zone of the northern Seram subduction, (iv) collision of two opposite dipping plates at the depth of their maximum penetration at about 400 km, (v) lack of seismicity beneath the Timor island. Earthquakes within the overriding plate are connected with magmatic activity beneath active volcanoes and with fault zones induced by the process of subduction.

Abstrakt

Příspěvek k tektonické interpretaci rozložení seismické aktivity v ostrovním oblouku Banda, jihovýchodní Asie

Tektonická stavba ostrovního oblouku Banda v jihovýchodní Asii je považována za mimořádně komplikovanou, protože oblouk se nachází v oblasti styku čtyř litosférických desek: Eurasijské, Indo-Australské, Pacifické a Filipínské. Současný tektonický režim oblasti je kolize ostrovního oblouku s kontinentem. Rozložení seismické aktivity v ostrovním oblouku Banda bylo studováno pomocí globálních seismologických dat. Byla použita relokovaná EHB hypocentrální určení za období 1964 – 2004 a ohniskové parametry harvardských CMT určení za období 1976 – 2004. Analýza prostorového rozložení zemětřesných ohnisek a ohniskových mechanismů umožnila oddělit ohniska náležející do Wadati-Benioffovy zóny subdukující desky od ohnisek náležejících do desky nadložní. Analýza vymezila dvě protiklonné subdukční zóny – jižní subdukci Banda a severní subdukci Seram. Ve Wadati-Benioffově zóně subdukující desky byla učiněna následující specifická pozorování: (i) neobvykle podélně zakřivená Wadati-Benioffova zóna jižní subdukce Banda, (ii) středně hluboká (100 – 220 km), svisle orientovaná doména s mimořádně vysokou seismickou aktivitou ve Wadati-Benioffově zóně jižní subdukce Banda, (iii) svisle orientovaný mělký seismicky aktivní segment s jednotnými přesmykovými ohniskovými mechanismy ve Wadati-Benioffově zóně severní subdukce Seram, (iv) kolize dvou protichůdně ukloněných desek v největší hloubce jejich průniku kolem 400 km, (v) zóna bez seismické aktivity pod ostrovem Timor. Zemětřesení v nadložní desce jsou spojena především s magmatickou činností pod vulkány a s aktivitou zlomových zón vyvolaných procesem subdukce.

Contents

List of Figures

Ráda bych na tomto místě poděkovala všem, kteří se mi věnovali při přípravě diplomové práce. Zejména RNDr. Aleši Špičákovi, CSc. za uvedení do problematiky deskové dektoniky a odborné vedení během zpracování diplomové práce a konzultantům RNDr. Václavu Hanušovi, DrSc. a RNDr. Jiřímu Vaňkovi, DrSc. za hodnotné připomínky. Dále bych jim ráda poděkovala za přijetí do kolektivu na Geofyzikálním ústavu AV ČR, v. v. i., kde mi poskytli prostředí a materiálovou podporu. Děkuji i Alici Guest za poskytnuté programy a Marii Běhounkové za pomoc s některými výpočty a všem ostatním, kteří mě podpořili a usnadnili mi vznik této práce.

Prohlašuji, že jsem svou diplomovou práci vypracovala samostatně s použitím citovaných pramenů. Souhlasím se zapůjčením práce.

V Praze, září 2008 Radka Matějková

1. Introduction

Significant progress in geosciences in the 20th century inferred the theory of plate tectonics developed in 1960s. Fundamental discoveries in two geophysical disciplines - paleomagnetism and seismology - contributed substantially to the concept of plate tectonics, among others. The plate tectonics concept has been comprehended in a paper by Isacs, Oliver and Sykes (1968).

A majority of the world's largest and most destructive earthquakes has tectonic origin, i.e. they are generated by motion of lithospheric plates along their margins. Very often, they occur at convergent margins of lithospheric plates, accompanied by volcanic activity, often in densely populated areas. On the other hand, convergent margins of subduction type give rise to beneficial products, such as ore deposits, geothermal energy, and the ground we live on. Subduction is the process by which one tectonic plate moves beneath another. It is also probably the most important mechanism by which lithospheric material is returned to the mantle and recycling of lithospheric material into the mantle has played a central role in the evolution of the crust and upper mantle. These are the reasons why it is so important to understand how subduction zones operate. Intensive investigation of convergent plate margins thus belongs to priorities in geosciences all over the world.

One of the most tectonically complex and recently active areas in the world is southeast (SE) Asia. This densely populated area was many times affected by disastrous events in the past (e.g. Tambora eruption 1815, Krakatau eruption 1883, Flores earthquake 1992, Sumatra-Andaman earthquake and tsunami 2004, Java earthquake 2006). The eastern closure of the region is formed by the Banda Arc which is the region of my interest (Figure 1). Here, the tectonic structure is extremely complicated as the Banda Arc is located at the intersection of four lithospheric plates: Eurasian, Pacific, Indo-Australian, and Philippine. Collision of Australia with the eastern Sunda and Banda island arcs represents a modern example of the early stages of arc-continent collision (Hamilton, 1979; Snyder et al., 1996b).

The geological setting of the Banda Arc provides a unique opportunity for studying the subduction of lithospheric material for the following reasons: pronounced seismic activity, intensive volcanic activity and many previous studies (geology, volcanology, geophysics, geochemistry, and geodesy).

In the last 30 years, the investigation of convergent plate margins based on seismological, volcanological, geological and tectonic evidence has been an inherent part of research in the Geophysical and Geological Institutes of Academy of Sciences. Systematic investigation of the geometry of distribution of earthquake foci at convergent plate margins (e.g. Tonga-Kermadec island arc, Andean South America, Mexico and Central America, Vanuatu island arc, Kamchatka, Kurile Islands, Hokkaido) resulted in the papers containing conclusions of general validity (Hanuš and Vaněk, 1976, 1978, 1981, 1985, 1991; Vaněk et al., 1987; Vaněk and Hanuš, 1988, 1990, 2000; Slancová et al., 2000; Špičák et al., 2004). In the last years, the research team has focused on the Sunda Arc, Southeast Asia (Hanuš et al., 1996; Špičák et al., 2002, 2005, 2007a). The goal of my work is to contribute to untangling the complexity of the Banda Arc dynamics.

High seismicity at convergent plate margins yields valuable data that are suitable to study their tectonic environment. One of the most efficient, straightforward and robust tools is the analysis and tectonic interpretation of spatial distribution of earthquake foci; this diploma thesis is based on utilization of this method. It serves to recognition of the present tectonics, deep structure, and, under suitable circumstances, also to interpret the tectonic history of subduction zones. The analysis of spatial distribution of earthquake foci enables to distinguish between events belonging to individual structural units and zones of weakness, and to correlate clustering of earthquakes with the position of volcanoes and faults. The tectonic interpretation of earthquake foci distribution must be always confronted with available geomorphological, tectonic, volcanological and geodetic data.

In the study of the deep structure of the Banda Arc region I have applied the methods of analysis and interpretation of the geometry of distribution of earthquake foci, which were used in the above cited papers, supported by parameters of available fault plane solutions.

2. Banda Sea region

The outermost part of the Earth consists of solid lithosphere of continental and oceanic type. The lithosphere is fragmented into lithospheric plates riding on the weak asthenosphere. Plate tectonics explains how these plates are created, move, interact, and are destroyed. The lithospheric plates move relative to one another along one of three types of plate boundaries: transform, divergent, and convergent. When the plates move along each other it is a transform or conservative boundary. Divergent or constructive boundaries are found along mid-oceanic ridges where new oceanic crust is created and plates move apart from each other. This process is called seafloor spreading. The third type, convergent margins, is destructive because two plates collide. When two continental plates collide, neither one can sink because both plates are similarly buoyant; this action creates extensive mountain ranges. The collision of dense oceanic plate with a less-dense and thicker continental plate causes subduction of oceanic plate underneath the continental one. When two plates with oceanic crust converge, an island arc is created as one plate is subducted below the other. The lateral movement of the plates occurs at present at velocity of 0.5 to 10 centimeters per year.

One of the common features of all types of plate boundaries is the occurrence of earthquakes within the lithosphere along the plate margins. In the subducted lithosphere, earthquakes are observed to depths down to 700 km. No earthquakes have ever been observed deeper in the lower mantle, but it does not mean that subducted plates could not penetrate into the lower mantle.

Seismic activity indicates deformation along plate and microplate boundaries. Another way to indicate plate boundaries and/or plate motions are paleomagnetic measurements and modern methods of satellite geodesy (Global Positioning System GPS, Very Long Baseline Interferometry VLBI and Satellite Altimetry). Geodetic methods enable to determine the direction and velocity of moving plates. The strain rate, deformations along the boundaries and the total rate of area production/destruction are then computed. The GPS gives the time information about current plate movements and of the motion at faults. In general, relative motions of lithospheric plates are defined by Euler geometry as a rotationary motion around the pole laying at Earth's surface. A final set of present plate boundaries on the Earth was gained from combination of topography, seismicity, volcanism, magnetic anomalies, moment tensor solutions for earthquakes, and geodesy. From these data there was established the International Terrestrial Reference Frame (ITRF, http://www.iers.org/MainDisp.csl?pid=42-17) which is constantly being updated. NUVEL-1A is an international standard model of ITRF (De Mets, 1994; Jin and Zhu, 2004). At present, 14 large plates and 38 small plates are described by the NUVEL-1A model (Bird, 2003) which distinguishes 7 types of plate boundaries: continental convergence zone, continental transform fault, continental rift, oceanic spreading ridge, oceanic transform fault, oceanic convergent boundary, subduction zone. Paleomagnetic methods measure the ocean-floor magnetic stripping record to calculate paleotectonic movements of regional range. The configuration of microplates is extremely complex and its reconstruction is very difficult. Therefore various interpretations of plate motions more or less differ.

The region of the Banda Arc lies in Southeast Asia (Figure 1), approximately between coordinates 2°S and 10°S and between 124°E and 135°E, where a part of Republic of Indonesia is situated. The arc resulted from the collision between the Eurasian, Indo-Australian, Philippine and Pacific plates at the SE margin of the Eurasian plate (Figure 1). The Banda Arc measures about 2400 km from Timor along the trench and is sharply curved on the east, the outer diameter of the bend being 500 km. Eurasia is considered to be the steadiest of all plates; it moves 2.4 cm/yr SE. Australia moves 7.1 cm/yr NNE, Philippine Sea plate moves 7.1 cm/yr W, and Pacific plate moves 6.2 cm/yr W – all values are relative to 5°N, 129°E in Eurasia (McCaffrey, 1996; DeMets, 1994; Plate Motion Calculator at http://ofgs.ori.u-tokyo.ac.jp/~okino). The Australian and Philippine plates subduct beneath the Eurasian plate.

The largest present-day tectonic block in the Indonesian region - the Sunda plate or Sunda block - represents a continental shelf of maritime SE Asia. SE Asia and Sunda block may significantly move relative to the rest of Eurasian plate due to the collision of central Asia with India (Bock et al., 2003). Because the motion of SE Asia relative to the rest of Eurasia is poorly constrained, SE Asia is treated as a part of Eurasia (McCaffrey, 1996, Hinschberger et al., 2005). The velocity field derived from GPS surveys shows several distinct tectonic regimes dividing the region into 4 small plates: Banda Sea, Molucca Sea, Timor, Bird's Head (Bird, 2003). An alternative division is suggested by Bock et al. (2003): Sula block, South Banda block, Bird's Head block; a very detailed division to 40 microplates is proposed by Hinschberger et al. (2005).

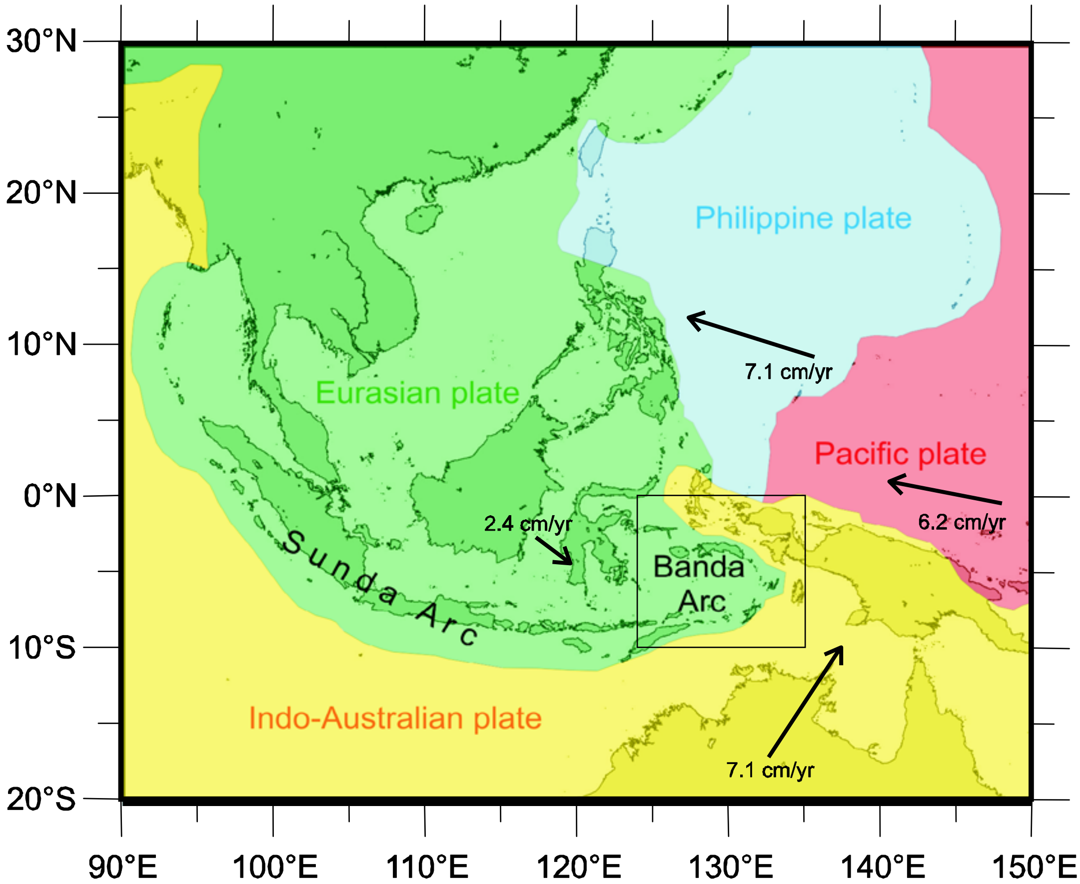

Figure 1. Main tectonic plates in SE Asia. Arrows indicate the direction and velocity of plate motion (DeMets, 1994). Rectangle indicates the Banda Sea region displayed in Figure 2a.

2.1 Morphology

Island arc, an oceanic type of volcanic arc, is composed of oceanic trench, non-volcanic and volcanic arcs, and a back-arc system, distinguished largely on the basis of topography and bathymetry. Island arcs have characteristic features in common: recent volcanic activity, deep-sea trenches and deep earthquakes. The trace of the subduction system follows the trench that is the deepest part of the ocean floor. As the oceanic plate approaches the trench, it is first moderately bent upwards and then descends to form the outer trench slope. The steeper inner slope of the trench is above the place where the two plates slide past each other. The frontal part of the overriding plate is usually in the form of an accretionary wedge; it is formed due to a high bed of sediments. The overriding plate contains a volcanic arc and a fore-arc. Volcanic arc (or volcanic chain) and accretionary wedge (non-volcanic arc or fore-arc) are separated by a fore-arc basin (synonym an outer-arc trough).

Island arc is an important structural feature of the Banda Sea region with several significant morphological peculiarities. The sharp curvature is the most characteristic pattern. No other island arc in the world is bent by about 180°. The morphology of the Banda Sea region (Figure 2a) will be described in the following order: from the outer features to the inner features and in the anti-clockwise direction from the southwest, around the bend, to the northwest.

The Banda Arc is surrounded by the trough with relatively shallow water depths (1 – 3 km). In the south and southeast there are the Timor-Tanimbar troughs, then the Aru trough in the east around the sharpest bend reaches the depth over 3 km, similar to the Seram trough in the north. The troughs are underlain by the Australian continental crust up to 40km thick and covered by sediments (Hamilton, 1979). In comparison with the fore-arc basin, the Weber basin is much deeper than the troughs. The fore-arc basin between the volcanic and non-volcanic ridges is continuous around the arc, underlain by oceanic crust, and deep about 4 km whereas the Savu Basin and the Weber Basin are wide and exceed much greater depth (6 and 7 km, respectively; Figure 2b,c and d). This is another not typical feature of the island arc: the fore-arc basin is deeper than the trench. In comparison with the Sunda Arc: the Java trench is deeper than 7 km whereas the Java fore-arc basin reaches the depth of about 3 km.

The fore-arc ridge forms many islands, interpreted to consist of Tertiary subduction melange and imbricated complexes, overlain by upper Neogene sediments (Hamilton, 1979). The largest islands of the arc are Timor, Tanimbar, Kai islands, Seram and Buru. Mud volcanoes are also common as a product of the rapid tectonic burial of wet sediments within the melange wedge. The non-volcanic fore-arc is a geologically complicated topographic ridge (Katili, 1989) where some islands exceed the dimensions of typical fore-arc islands, especially Timor.

In the western islands of the southern limb of the inner volcanic arc, there are presently inactive volcanoes Alor, Wetar, and Roma (or Romang). At the curved eastern part of the arc active volcanoes Damar (or Wurlali), Teon, Nila, Serua, Manuk, and Banda Api occur. The ridge is otherwise marked by submarine seamounts, which appear to be volcanoes, especially in the northern limb of the arc. Igneous activity started at least 12 Ma ago above the subducting slabs (Snyder et al., 1996b). The volcanic arc consists primarily of Neogene and Quaternary calk-alkaline

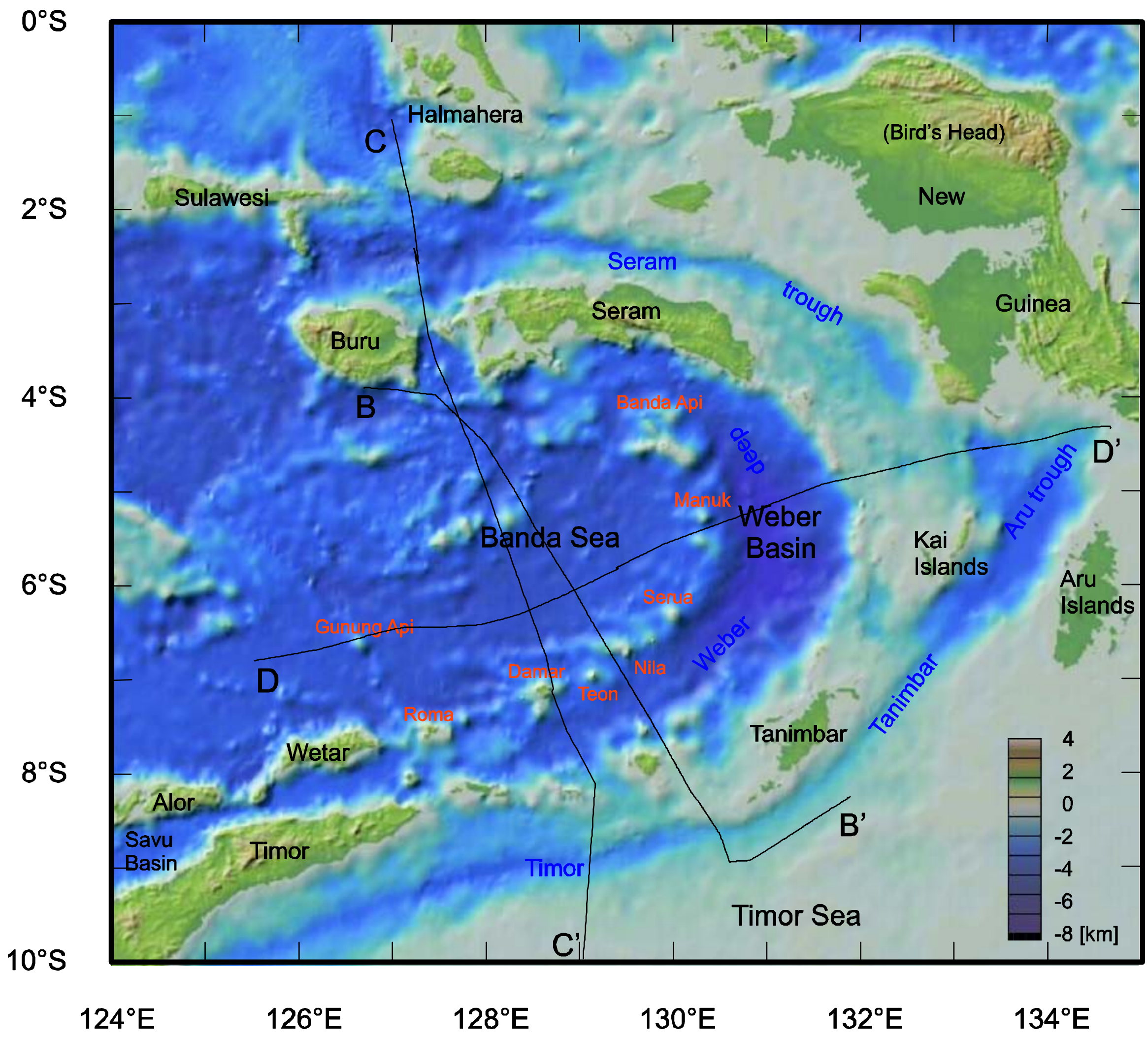

Figure 2a. Morphological map of the Banda Sea region. Lines BB', CC' and DD' indicate the cross sections in Figures 2b, c and d.

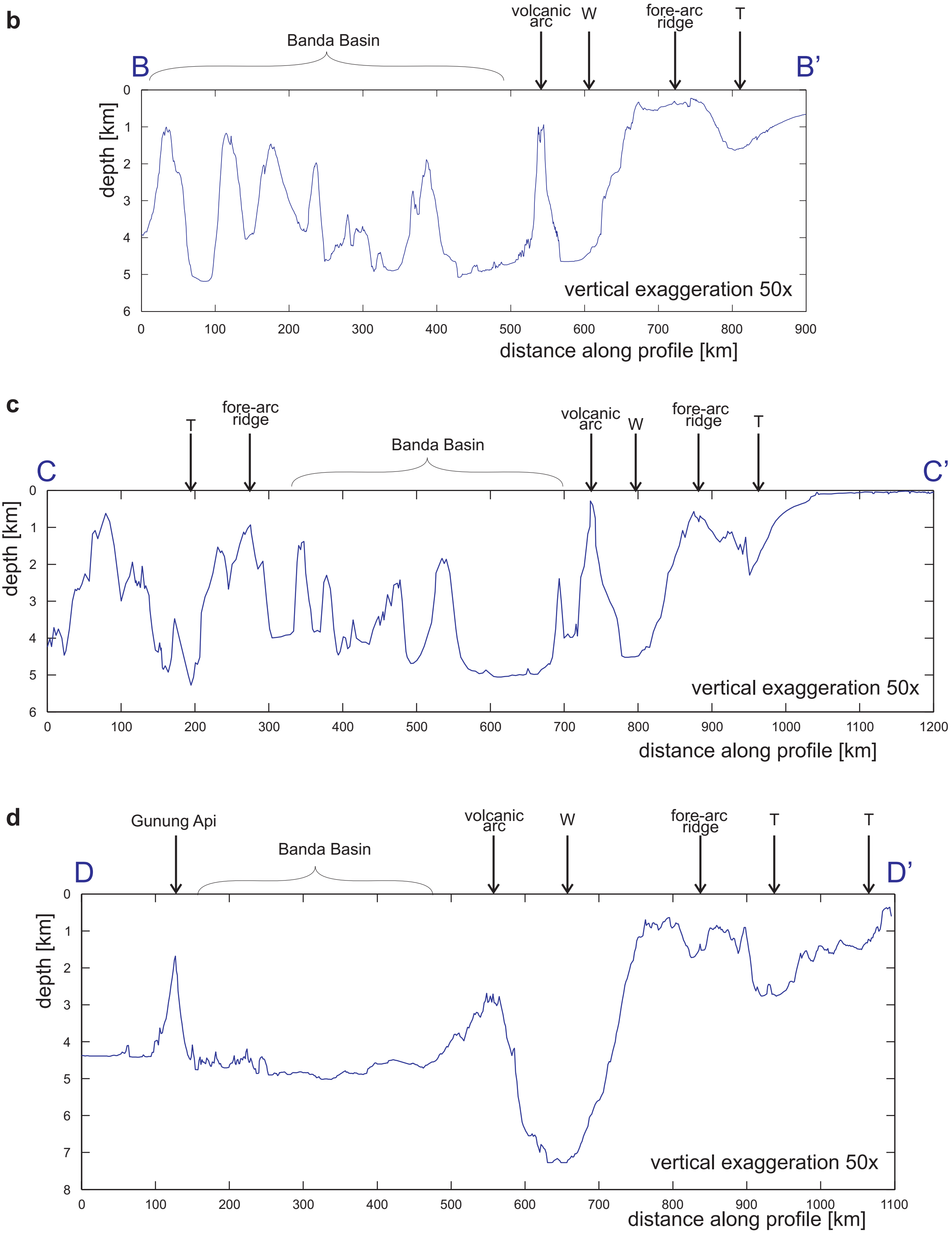

Figure 2b, c and d. Seafloor topography of sections across the Banda Sea region. Location of the sections is shown in Figure 2a. The sections are parts of ship tracks: b cruise A2093L13, c cruise V2008, d cruise INDP14WT (http://maps.continentalshelf.org/geodas/). Data are available at http://www.geomapapp.org.

volcanism (Hamilton, 1979), but rock types change from low-K tholeitic in the NE to high-K calk-alcaline in the SW. The volcanoes of the northern limb have normal arc signature, whereas those in the southern limb have anomalously high content of K-components (Vroon, 1992).

At the western part of the Banda Sea, north of Wetar, Gunung Api volcano and a chain of submarine seamounts can be found oriented N 160° E (Figure 2a). Gunung Api is a volcano composed of lavas which are similar to those of the South Banda Arc volcanics (Vroon, 1992). The line of seamounts coincides with a transform fault called Gunung Api fracture zone (Snyder et al., 1996a; Hinschberger et al., 2003) which has acted as a magma conduit. The location of this fracture may be due to an older zone of weakness and is presently affected by a left-lateral strike-slip reactivation (Snyder et al., 1996b; Hinschberger et al., 2003, 2005).

The most significant morphological structures of the Banda Arc are the volcanic arc, the Weber deep and the trench. The line of the volcanic arc and the axis of the fore-arc ridge are parallel and 60 to 100 km apart. The distance of the volcanic arc and the trough varies. In the Timor trough it varies from 180 to 230 km, in the Tanimbar trough it is about 270 km, at Aru trough 380 - 400 km, and at Seram trough 200 - 300 km. The limit of the Australian continental crust is parallel to the trough according to Hamilton (1978) at the distance of 100 - 150 km except the eastern curved part, where the distance is about 200 km. Generally, the distances are smallest at the southern limb across the Timor island and largest at the eastern part of the greatest curvature of the arc.

Forming a morphological curve over 180°, the arc encloses the South Banda Basin of the Banda Sea underlain by oceanic crust with typical thickness of 11 km (Snyder et al., 1996a). Water depth in the Banda Sea is 3 - 5 km, with ridges and seamounts rising 2 km above the sea floor.

2.2 Tectonic Evolution

All lithospheric plates move relative to their neighbors so that the plate boundaries, including trenches, change their shape and move also. The tectonic configuration of the Banda Sea region thus underwent several significant changes in the past.

Stratigraphic, geological, paleontologic, and paleomagnetic comparative studies in the East and Southeast Asia reveal that these regions were directly or indirectly detached from Gondwanaland (Metcalfe, 1996). The motions of major plates through the Tertiary period are reasonably well understood, being constrained by ocean floor magnetic anomalies and by other paleomagnetic data (Daly et al., 1987). The break-up of Australia from Antarctica has most recently been estimated as mid-Cretaceous (95+/-5 Ma; Hall, 1996). Australia moved eastward, but collision of India and central Asia caused a change of the direction northward when a rapid ocean-floor spreading began in the southern Indian Ocean (about 50 Ma ago). In consequence of a marked change in the motion of the Pacific plate from NNW to WNW (about 42Ma ago), the Philippine Sea plate was separated. The Philippine Sea plate consists entirely of oceanic crust bordered by an island arc system and has been moving W to NW with respect to Eurasia, as is the case today, and a large part of it has been subducted beneath the eastern Eurasian margin (Daly et al., 1987). Another collision occurred at about 25 Ma ago (late Oligocene) when an oceanic island arc originated in the southern margin of the Philippine plate and collided with the northern margin of the Australian continent. In Miocene, small islands along the present-day Banda Arc bend were striking east-west (Katili, 1975). At 11 - 5 Ma ago, collision of the Bird's Head microcontinent with Papua New Guinea caused a detachment of microcontinents that escaped westwards along the Sorong Fault. In Pliocene, the western part of the Banda Arc joined the eastern Sunda Arc and the eastern part of the Banda Arc was bent westward as Australia moved to the north. The Banda Sea is interpreted to have an extensional origin and to have opened during the late Neogene (Hall, 1996). There were three oceans destroyed by subduction of Australian plate beneath Eurasia: Paleo-Tethys, Meso-Tethys and Ceno-Tethys were opening and closing by the northward drift of Australia.

A new tectonic regime appeared when the collision between the Australian margin and the Banda Arc subduction system occurred in Neogene; this process has been also called the Banda orogeny (Richardson and Blundell, 1996). This arc-continent collision and its age is an issue of controversy. The subduction of the Australian continental lithosphere is estimated starting in the Late Miocene – Early Pliocene, at least 3 Ma ago (Tandon et al., 2002). The full collision of Australian continental shelf with Banda arc is dated to about 2 - 2.2 Ma ago (Snyder et al., 1996b), but the continental material entered for the first time into subduction process 8 Ma ago (Snyder et al., 1996b). A continued northward movement of the Australian continent has been accommodated by an uplift of the collision complex in Timor and by lateral extension along conjugate faults. At present, the subduction within the Timor trough stopped and the majority of strain is being accommodated within the fore-arc basin and the back-thrust fault zone (Tandon et al., 2002).The Banda Sea was thought to be an old entrapped oceanic crust (Katili, 1989) but recent work has shown that it was formed by a back-arc extension during the Late Miocene – Early Pliocene time (Hall, 1996; Hinschberger et al., 2001).

2.3 Previous investigations

In SE Asia, many surveys and investigations were carried out in the framework of petroleum prospecting, mining of mineral resources, and special studies on the geological setting of the region. Indonesia has extensive natural resources, including crude oil, natural gas, tin, copper, and gold, and extreme seismic and volcanic hazards.

In the past decades expeditions have used the modern technology (e.g. satellite altimetry, deep sea drilling) to obtain more precise data. These surveys have provided a wealth of information about structures in the uppermost 5 km of the crust (Snyder et al., 1996b). Information about crustal-scale structures like faults and shear zones can be provided by global teleseismic studies, refraction profiling, and regional gravity surveys. However, information about the mantle structure in subduction zones can be obtained only by analysing the seismic data.

From 1970’s the Indonesian region has been regarded as a continental margin and surveys were adapted to it. Multiparalel studies in local and/or regional scale became the basis for many scientific studies and maps. Geology and plate tectonics of SE Asia was discussed by Fitch and Molnar (1970), Fitch (1970), Katili (1975), Audley-Charles (1975, 1981), McCaffrey (1989) and others; the most complex works should be stressed: *Tectonics of the Indonesian region* (Hamilton, 1979), *Tectonic map of Indonesian region* (Hamilton, 1978), and *Tectonic evolution of Southeast Asia* (Hall and Blundell, 1996). Paleoreconstructions of SE Asia have been presented e.g. by Daly et al. (1987), Packham (1996), Hall (1996, 2002).

Despite numerous studies of the Banda Sea region, no unifying theory has been proposed for the tectonic evolution of the Banda Sea region. The plate tectonics of this part of Indonesia was discussed by many authors, partly on the basis of the distribution of earthquake hypocenters, as well as geological and geophysical data, partly on studies of focal mechanisms. Previous studies of the geometry of the subducted lithosphere beneath the Banda Sea have led to conflicting views on the shape of the slab(s) beneath the Banda Sea largely due to a lack of well-recorded deep earthquakes available when those studies were made (McCaffrey, 1989). The only thing with which authors have agreed is that the structure is complicated as a result of several plate collisions and requires a separate detailed study (Schöffel and Das, 1999). Often their conclusions were made on the basis of one method without correlation with other measurements and observations.

From 1970's the Banda Sea region has been regarded as an island arc and the first idea was the model of one subducting plate contorted around the Banda Arc (Fitch, 1970; Fitch and Molnar, 1970; Katili, 1975; Audley-Charles, 1975). These papers were based on geological prospecting, later on analysis of earthquakes, however the former datasets were less extensive and less precise than the present datasets and only a few focal mechanisms were available (McCaffrey, 1989).

The Banda Arc is characterized by a spoon-shaped Wadati-Benioff zone that dips inward from the south, east, and probably north to depths that exceed 600 km beneath the western Banda Sea (Hamilton, 1979). However, McCaffrey (1988) concluded that it is geometrically incompatible for the Australian plate to subduct simultaneously beneath both the Timor and Seram troughs. Cardwell and Isacks (1978) showed that it is difficult to imagine a subduction around a 180° bend without a disruption of the plate. With a simple laboratory test they found that it is not possible to deform a single lead sheet into a continuous loop-shaped subduction zone extending from Java to Buru. Instead, they suggested a model of two lithospheric plates descending into the upper mantle beneath the Banda Sea. The major one descends toward the north beneath the Banda Arc to a depth of 600 km; the second one descends toward the southwest in the region of Seram to a depth of about 200 km. An abrupt change in the trend of seismicity of the Banda Arc can be found at the eastern part of the arc (Das, 2004; Hinschberger et al., 2005). These two adjacent, oppositely dipping subducting plates are connected by the left-lateral strike-slip Tarera-Aiduna fault zone, which acts as an arc-to-arc transform fault (Cardwell and Isacks, 1978).

The conclusions of Cardwell and Isacks (1978) were confirmed by a tomographic study by Widiyantoro and van der Hilst (1996, 1997) who used the EHB dataset (after **E**ngdahl, van der **H**ilst and **B**uland, Engdahl et al., 1998 – for the detailed description of the EHB dataset see below Chapter 3.2.2, page 20), referenced velocity model ak135, and approximately equal area blocks of 5° x 5° and 1° x 1° within the study region. Their inversion suggests a twisting of the slab in the upper mantle, which parallels the present-day curved Banda Arc and that represents a pronounced seismic anomaly in the lower mantle (at least to 1500 km depth). The model of two slabs was also supported by Hamilton (1979), McCaffrey (1989), Ritsema et al. (1989), Pustito and Shimazaki (1995), Das (2004) and others.

2.4 Present-day tectonic setting

The complicated structure beneath the Banda Sea region is mainly due to its curved morphology and collision with the northward-moving Australian continental shelf. The tectonic setting of the region influenced the distribution of stress along the arc. Stress conditions vary along the arc: the Timor and Seram troughs show compressional and the Aru trough extensional regime (Katili, 1989). The northward motion of Australia causes a horizontal shortening across the convergent zone because the Timor trough cannot absorb the continental lithosphere as easily as the oceanic lithosphere (Snyder et al., 1996a). The present-day tectonic regime is characterized by the following phenomena: shortening in the direction of convergence (north-south direction), elongating in the direction perpendicular to convergence (east-west direction), and thrusting over the back-arc basin (McCaffrey, 1988; Milsom et al., 1996). The arc-continent collision is in an early stage (Snyder et al., 1996b). This collision has commenced in the region that is now East Timor (Timor collision); it is at its most advanced stages in this segment of the arc. Beneath Timor, no intermediate-depth earthquakes occur, which means that the subducted slab is locked in this part of the arc (Simandjuntak and Barber, 1996) and the subduction regime transforms to the collision regime. The eastern limit of the Sunda Arc Wadati-Benioff zone at longitude 125°E and the western limit of the Banda Arc Wadati-Benioff zone at longitude 127°E can be delimited (Špičák et al., 2007a). The continental lithosphere is supposed to be unsubductable due to its buoyancy and low density (McCaffrey et al., 1985; Hamilton, 2002). The cessation of volcanism and a change of chemical composition of magma are evidences of the collision and indicate the presence of the continental lithosphere in the subduction zone. The extinct volcanism north of Timor indicates that the subduction probably terminates there. The contamination by continental crust material is demonstrated by chemical composition of magma. Rock types change from low-K tholeitic (Banda Api) in the NE to medium-K (Manuk, Serua) and high-K (Nila, Teon, Damar) calk-alcaline in the SW (Vroon, 1992). The continental crust material (rich in K-components) has been subducted to 150 km depths where it has melted and contaminated the rising magmas (Audley-Charles, 1981; Snyder et al., 1996a, 1996b). Banda Arc magmas result from mixing of three source components: a mantle component, subducted continental material and fluids (Vroon, 1992). However, chemical analysis of magma cannot unambiguously confirm if the magma components can be either subducted continental crust or detrital sediments derived from it before subduction (Vroon, 1992).

On the basis of a detailed study of focal mechanisms, some authors suggest that a part of the subducting plate may have started to disconnect from the continental part in the collision zone (McCaffrey et al., 1985; Charlton, 1991; Tandon et al., 2002). These two facts – subduction of the continental crust and disconnection of the subducting plate from the continental part - are regarded as causes of rapid uplift and upfolding especially of Timor and are evidenced by several hundred meters of elevation of Pliocene coral reef terraces (Richardson and Blundell, 1996). Earthquake distribution suggests that the present stage of collision of the Australian continental margin with the Banda Arc probably involves more rapid convergence at the back-arc thrust than at the Timor trough (McCaffrey et al., 1985; Hamilton, 1979; McCaffrey, 1996; Tandon et al., 2002). The contact between the inner volcanic-arc ridge at Alor and the south edge of the South Banda basin is a young, south-dipping subduction system named Wetar thrust. Here is the north boundary of the Timor microplate (Bird, 2003; Bock et al., 2003) which has been separated from Sunda block and now moves with the velocity closer to that of Australia than that of Sunda.

The Timor, Tanimbar and Aru throughs are interpreted as an oceanic trench of subduction zone separating the Australian and Eurasian plates (Hamilton, 1979); however, some authors argue that no subduction has occurred between Australia and the outer Banda Arc. Fitch (1970), Fitch and Molnar (1970) considered the Weber deep as an oceanic trench. Audley-Charles (1975) compared the morphology of the Weber deep and the Timor-Tanimbar-Aru troughs with the morphology of the Java trench and speculated whether the Weber deep could be a subduction trench. It was found that the most active tectonic center is related to the most curved part of the arc, indicating that the deformation of the lithosphere is strongest there (Papp, 1980). Here is the deepest structure of the arc – the Weber basin. And the question is if it could be so deep resulting only from extensional tectonics. Katili (1975) suggests that the Weber deep is a relict of an old subduction and has both the subduction and extensional origin. The Timor-Tanimbar-Aru through is also regarded as a foredeep at the front of a developing fold belt (Tandon et al., 2002; Pairault et al., 2003). The function of the troughs is still debated.

The Seram trough in the north has been the subject of controversy as to whether it is a subduction trench (Hamilton, 1979), a zone of intraplate shortening (Tandon et al., 2000, Pairault et al., 2003) or a strike-slip zone (Milsom et al., 1983). Beneath the Seram trough and Seram island there is a south-dipping slab subducted in the past and considered as a part of the Australian, later as a part of the Pacific plate. The Seram trough and the Pacific plate are separated by Bird’s Head which has been a part of Australian plate (Puntodewo et al., 1994). The westward migration and anti-clockwise rotation, resulting from the combination of the northward movement of the Australian plate and the westward movement of the Pacific plate, made the Bird’s Head a separate microplate (Bird, 2003; Bock et al., 2003). A study of new seismic lines shot across the Seram trough favors a foredeep model although a subduction origin cannot be completely excluded, but there is no evidence of strike-slip faulting (Pairault et al., 2003). The Seram trough is now generally agreed to be the site of southward underthrusting of the Bird's Head as indicated by earthquake mechanisms (McCaffrey, 1989).

The most pronounced fault zone of the region is the Sorong fault zone. The west-east oriented faults of the fault zone between 1°S - 2°S and 125°E - 140°E have accommodated the convergence between the Australian and Pacific plates by a strike-slip motion (Puntodewo et al., 1994). At present, its function transposes to the Tarera-Aiduna fault zone. The west-east oriented Tarera-Aiduna strike-slip fault is clearly visible as a linear feature on satelite images through New Guinea (Figure 2a) and continues toward the Banda Sea. It acts as a trench-to-trench transform fault (Hinschberger et al., 2005) between northern and southern subduction in the Banda Arc. The Banda Sea floor is cutted by several ENE-WSW fossil transform faults (Hinschberger et al., 2003).

At present, many national and international programs and projects are devoted to the investigation of geodynamics of convergent plate margins. The projects oriented to the reduction of seismic and volcanic hazard are emphasized, especially in the densely populated areas as Indonesia is. For disaster reduction in regions of high risk potential for the population, the projects as MERAPI or German-Indonesian tsunami early warning system were established. A goal of the interdisciplinary project MERAPI (Mechanism Evaluation, Risk Assessment, Prediction Improvement, http://www.gfz-potsdam.de/pb2/pb21/merapi/index.html) is to deepen the under-standing of volcanic processes and mechanisms, to improve the methods for volcanic risk estimation, to develop forecast strategies, and to bring the realizations into an early warning system for the Merapi volcano, Java, Indonesia. GITEWS (German-Indonesian tsunami early warning system, http://www.gitews.org) is a project of the German Government of the reconstruction of the tsunami-prone regions of the Indian Ocean. The concept is aimed at achieving indicators of a tsunami and its dimensions by the analysis of various measurements at an early stage of tsunami developement based on different kinds of sensor systems.

To study various expressions of volcanism and its relations to the active subduction environment are the aims of interdisciplinary projects monitoring volcanic activity of Krakatau, Merapi and Kelut: KRAKMON, MERAMEX, DEVACOM of Indonesian and

German partner institutions (http://www.cosis.net/abstracts/EGU04/ 06429/EGU04-J-06429-1.pdf

3. Data and Methods

3.1 Seismological data

In this diploma thesis, the seismicity pattern of the Banda Arc was studied by means of global seismological data. Global seismological data result from operation of the global, world-wide international network of seismic stations, gathered and assessed by several seismological centres, among which the International Seismological Centre (ISC) and National Earthquake Information Centre (NEIC, http://earthquake.usgs.gov/regional/neic/) are the most respected ones.

3.2 Hypocentral determinations

3.2.1 ISC data

The ISC (UK, http://www.isc.ac.uk/) is a non-governmental organization charged with the collection, analysis and publication of standard earthquake information from all over the world. The ISC currently produces two publications, the tri-annual *Bulletin of the ISC* and the semi-annual *Regional Catalogue of Earthquakes*. The *Bulletin* includes all earthquakes recorded by more than one independently operated network and contains all relevant information on each earthquake (including origin estimates by other agencies; a refined estimate by the ISC, with time, location and standard error; additional source information such as moment tensor solutions; for large earthquakes, associated phase arrival reports). In the *Regional Catalogue of Earthquakes,* hypocentral data of events are grouped by geographic regions (50 regions). The catalogue presents a comprehensive summary of hypocenters for all sufficiently large earthquakes (lists of m_b > 5.5 shallow and intermediate focus and m_b > 5.0 deep focus earthquakes), reports of felt and damaging earthquakes and probable explosions. Production of the printed catalogue ceased in 2004. Catalogue from 2001 is available in PDF format both on ISC CDs and on the ISC FTP site ftp.isc.ac.uk.

Earthquake readings are received in the ISC from over 4,000 seismograph stations from the entire world. To determine hypocentral parameters, P-wave travel-time tables derived from the radially stratified Jeffreys-Bullen (JB) Earth velocity model inferred from velocity models iasp91 and SP6 are used (Willemann and Storchak, 2001).

Lateral variations in velocity, uneven spatial distribution of seismic stations, magnitude-dependent observational uncertainties can easily combine to produce earthquake mislocations and errors in focal depth of several tens of kilometers. The influence of mislocations and errors can be significantly reduced by limitating only to those events that are well constrained. More accurate dataset of the ISC hypocentral determinations can be achieved by a simple filtration: hypocentral data characterized by standard errors in epicentral coordinates greater than 0.2° and by observations with epicentral distances smaller than 20°, are filtered out. The reduced dataset is exploitable for detailed seismotectonic studies (e.g. Hanuš et al., 1996).

Relocation is a way of improvement of the dataset of ISC hypocentral determinations. Relocation procedure is a computation of hypocetral determinations which uses the readings published by ISC and changes input data - adds some later-arriving phases and uses a different reference Earth model. At present, EHB dataset (after **E**ngdahl, van der **H**ilst and **B**uland; Engdahl et al., 1998) is the most often used dataset of relocated hypocentral determinations.

3.2.2 EHB data

Relocation procedure of Engdahl et al. (1998) improves some of the ISC and NEIC hypocentral determinations. The procedure (i) selects only events that are well-constrained teleseismically by arrival times reported to ISC for which the largest teleseismic open azimuth is less than 180°, and reported arrival times for some of first-arriving P and S phases, PKiKP, PKPdf, and the depth phases pP, pwP, and sP, which have been reidentified, (ii) uses the ak135 Earth model, an improved iasp91 model. Ak135 was designed as a representative of continental ray paths. Because most seismic stations lie on continents, it is optimum to use the ak135 model. Procedure includes operations as: travel-time corrections, phase identification, weighting, event selection, and event classification. The median difference for all

EHB epicentres relative to ISC epicentres (excluding shift >40 km) is 7.6+/-5.5 km with no obvious dependence on focal depth. The median shift for all EHB depths relative to ISC depths (excluding depth differences >40km) is -1.7+/-11.8 km. For events with depths less than 70 km, the median depth difference is small, but for larger depths, the differences are 3 to 4 km and negative.

Each event in the EHB database has a tag distinguishing among 7 classes of solution accuracy: (1) DEQ - the most common tag represents high accuracy of hypocentral determination with standard error in depth less than 15 km; (2) LEQ - depth of the event fixed by program with standard error in depth greater than 15 km; (3) FEQ - depth of the event fixed by Engdahl to the most probable depth; (4) BEQ - depth of the event fixed at the depth determined from broad-band observations; (5) WEQ - depth of the event fixed at waveform depth; (6) HEQ and (7) XEQ are the least accurate data. The letter Z is added to the tag when teleseismic azimuth gap of observations is greater than 180°. DEQ events form 65% of the EHB database. For more detailed and precise studies, a selection of DEQ data is suitable. The authors of EHB database do not recommend using any poorly located XEQ and Z events; they are listed for the information only. When constructing vertical sections, one should not use events that are poorly located in depth - LEQ events.

The EHB database for the period 1964 - 2004 is homogeneous for earthquakes with moment magnitude M_w>5.2 and includes all events for which moment-tensor solutions are available. These data represent about 15% of the total number of events of the ISC database. The EHB database offers altogether 2961 events located in the Banda Sea region bounded by coordinates 0° - 10°N and 124°E - 135°E during the period 1964 - 2004. Number of selected EHB events according to accuracy of hypocentral determination expressed by the EHB tag is given in Table 1.

Table 1. Division of events of the Banda Sea region dataset according the quality tag and number of focal mechanisms (HCMTS).

	Number of events	%
Banda Sea region dataset	2961	100
DEQ	1885	63.7
LEQ	701	23.7
FEQ	317	10.7
BEQ	56	1.9
HEQ,XEQ	2	0.1
WEQ	0	0
Z	3	0.1
HCMTS	592	20

The EHB data cover the time interval of 41 years, beginning with 1964, and represent a database with small random and systematic errors. The data accuracy appears to be sufficient for seismotectonic studies on a global scale. The homogeneity of database enables to reveal the decisive trends in seismotectonics of individual convergent plate margins and to define their general phenomena on the one hand and specific features typical only for a particular area on the other hand. The dense earthquake occurrence in both time and space enables to determine not only basic parameters of large tectonic structures as WBZ of subducting slabs, but also to study seismically active structures in lithospheric wedges above active subduction zones. The size of investigated structures in comparison with data accuracy makes the global seismological data as an optimum material for this work. The EHB data are accessible on request from the first author and consequently their utilization is inexpensive.

Apart from above mentioned global catalogues, catalogues of local earthquakes exist in many regions. They are usually results of short time recording of local networks of stations located in seismically active regions for the purpose to obtain more detailed information. These experiments are comprehensive, including weak to strong earthquakes, but needn't record significant trends of seismicity due to a short time interval of observation and limited area covered by seismic stations.

3.3 Focal mechanism data

Besides the main hypocentral parameters (the origin time, epicentre location, focal depth and magnitude), significant characteristics of an earthquake are focal mechanism, seismic moment, and moment tensor. From the moment tensor inversion, it is possible to resolve the orientation (strike and dip) of the plane and sense of slip (rake or slip) along the fault. Strike ϕ is the angle between outcrop of the fault plane and the north measured clockwise. It is that one of the two horizontal directions for which the fault plane dips on the right, as viewed by an observer looking along strike. Dip δ is the angle of the dip direction of the fault plane from horizontal plane. Rake λ is the angle between strike direction and slip within the fault plane. The possible types of faulting involved in an earthquake are: strike-slip, reverse (or thrust), normal, and their combinations.

A graphic expression of the focal mechanism is known as a so called beachball diagram. It is represented by focal lower hemisphere that is cut by two mutually perpendicular planes, called the nodal planes, into 4 quadrants. Two opposite ones represent compressional quadrants and are coloured black; remaining ones are dilatational quadrants and are coloured white. The compressive axis P (for the maximum compressive stress σ_1) is in the middle of dilatational quadrants, and the tension axis T (for the minimum compressive stress σ_3) is in the middle of compressional quadrants. One of the nodal planes is the fault plane, and the other is the auxiliary plane and has no structural significance. It is impossible to say which one of the nodal planes is the fault plane. However, additional information as distribution of aftershocks or geologic and geodetic information can help to distinguish between the two possible planes.

The analysis of available focal mechanisms results from the conception that the tectonic earthquakes are shear events and their focal mechanisms are represented by a double couple (DC). Parameters of nodal planes and eventually of P-axis are used to constrain the tectonic regime, state of stress, detailed internal structure of subduction zone as well as individual clusters of earthquakes and the geometry of a fault rupture.

3.3.1 CMT solutions

Moment tensor determination from available teleseismic and/or regional data has become a routine procedure in seismology. The focal mechanism solutions are determined by several centres, from which NEIC (http://neic.usgs.gov/neis/FM/) and Harvard CMT Project (http://www.seismology.harvard.edu/projects/CMT/) are the most reputable; their results have usually no significant differences. One of the activities of the Harvard Centroid Moment Tensor (CMT) Project is systematic and fast determination of centroid moment tensor for strong earthquakes with M>5.5 over the period from 1976 till present and accumulation of the results in the extensive CMT catalogue.

The standard ISC/EHB hypocenter location corresponds to the place where rupture started. Therefore, the offset of the centroid location relative to the hypocentral location can give the first indication on rupture directivity. The median difference for all EHB epicentres relative to CMT centroid epicentres (excluding epicentral differences > 100km) is of the order of 30 km or more, regardless of the depth range (http://www.globalcmt.org).

Selection from the datasets EHB 64 - 04 and HCMTS 76 - 04 for the Banda Sea region is appended on CD (Appendix 2).

3.4 Methods and applications

Among the most powerful tools offered by seismology that are available for the study of subduction zones and for the analysis of causes of seismic activity belong: (i) seismic tomography; (ii) numerical modelling of subduction process; (iii) determination of moment tensor and its interpretation; (iv) analysis of spatial distribution of earthquake foci; (v) tectonic analysis of routinely calculated available focal mechanisms.

(i) Seismic tomography provides a 3-D model of Earth's velocity structure. This method is able to detect velocity heterogeneities of size of about 100 km in the upper mantle; therefore it is not suitable for detailed study of the internal structure of the subduction zones. If useful, any sections for our studies will be provided on request from Prof. Wim Spakman and his research group, Department of Earth Sciences, Utrecht University, the Netherlands.

(ii) Numerical modelling of the process of subduction is the domain of our partners at Department of Geophysics, Faculty of Mathematics and Physics, Charles University in Prague (e.g. Čížková, 2005). This approach enables to estimate under which conditions subduction occurs.

(iii) Moment tensor determination leads to a complete description of equivalent forces of a general seismic point source. By the moment tensor decomposition, isotropic part (ISO) and deviatoric part (DEV) are obtained. DEV incorporates shear component DC and the rest is compensated linear vector dipole (CLVD) which represents non-shear component within the ISO part.

The determination of CMT directly from seismograms from local seismic stations is one of the domains of Institute of Geophysics, Academy of Sciences of the Czech Republic (http://www.ig.cas.cz/en/seismic-service/seismic-bulletins) and Department of Geophysics, Faculty of Mathematics and Physics, Charles University in Prague.

The determination of CMT directly from seismograms and the tectonic interpretation of shear and non-shear components of seismic source would become an item of my postgradual studies.

(iv) and (v) The analysis of spatial distribution of earthquake foci and tectonic analysis of routinely calculated available focal mechanisms are the fundamental method in this thesis. Their detailed description will follow below in Chapter 3.6.

3.5 Geological data

The information on volcanoes was taken from the Volcanoes of the World (Simkin et al., 1981), Volcanic activity Reports (Venzke et al., 2002), and Global Volcanism Program (http://www.volcano.si.edu/gvp). The geological and tectonic information is taken mainly from Tectonic map of Indonesian region (Hamilton, 1978) and numerous papers (see References). The sea-floor morphology was taken from GeoMappApp (http://www.geomapapp.org/). The geodetic information was taken from Plate Motion Calculator (DeMets et al., 1994).

3.6 Analysis of global seismological data

The fundamental method used in this thesis is the analysis of spatial distribution of earthquake foci. The distribution of earthquake foci at convergent plate margins is non-uniform; it reflects tectonic structure, tectonic stress concentration, brittle or ductile character of the medium and tectonic history. Earthquakes within subduction zones occur mostly in subducting slabs; these earthquakes visualize the seismically active part of subducting lithosphere that is called the Wadati-Benioff zone (WBZ). Significant seismicity is observed also in the lithospheric wedge above the Wadati-Benioff zone. These earthquakes are usually generated at large fault zones or beneath active subduction-related calc-alkaline volcanoes.

The computer techniques enable a 3D visualization of distribution of earthquake foci but size of a computer screen doesn't enable to visualize the distribution of earthquakes in sufficient scale. The relatively dense system of vertical sections is friendlier. Each section includes the group of earthquakes the epicentres of which are situated within a swath of a certain width. The width of swaths has to be chosen carefully; the choice mainly depends on the density of earthquake occurrence in the investigated region. Too narrow sections do not give a representative image of earthquake distribution whereas in too wide sections, lateral changes in earthquake distribution can be easily covered. There is no exact rule how to determine the width of sections; it is chosen empirically (50 km in most convergent plate margins).

The choice of section orientation is important to evaluate the spatial distribution of earthquakes properly. Differently oriented sections were used to study the distribution of earthquakes in the Banda Arc (e.g. McCaffrey, 1889; Das, 2004; Milsom, 2001). At subduction zones, the dominant structural element is the plate margin which is parallel to trench/trough and volcanic arc. Due to complicated structure of plate margins in the Banda Sea region, both two sets of sections were chosen perpendicular to the axis of the Timor, Aru and Seram troughs. The western part of the Banda Arc was covered by north-south oriented parallel sections, as both the Timor and Seram troughs are linear and east-west oriented in this part of the arc. The eastern, curved part of the Banda Arc was covered by a fan of triangular sections with the vertex at 5°S, 129°E as the Tanimbar-Aru-Seram troughs are bent by about 180° in this part of the arc.

Nine north-south sections 55 km wide (0.5 geographic degree) and 990 km long (9 geographic degrees) were constructed at the western part of the Banda Arc from longitude 126.5°E to 130.5°E. In the eastern, curved part of the arc, a fan of 15 trianglular sections were constructed with the vertex at 5°S, 129°E, vertex angle 10°, and the length of 605 km (5.5 geographic degrees). Location of the sections is shown in Figure 3: north-south sections are marked NS1 – NS9 (Figures 4 - 12) and triangular sections are marked according to their azimuth, az40 - az180 (Figures 13 - 27). The 25 sections in Figures 4 - 27 give the depth distribution of earthquake foci.

Another standard and useful tool in depiction of earthquake distribution is a longitudinal section along the slab, enabling to project the earthquake foci to the plane of the WBZ. It is suitable that the longitudinal section contains only those earthquake foci belonging to the WBZ. The dip of longitudinal section should be chosen parallel to the slab, allowing delineating the lower limit of the WBZ and the position of aseismic gaps. Then the y-axis in Appendix 1 and Figure 28 gives the distance down-dip along the subduction, with zero value at the Earth surface. To relate the position and mechanism of events directly to the medium of their occurrence, focal coordinates and fault plane parameters of events in this domain were transformed to the plane defined by parameters characterizing the WBZ (Appendix 1).

The longitudinal section along the Timor-Tanimbar-Aru troughs was constructed projecting the earthquake foci to the plane of the southern WBZ (Appendix 1). The surface trace of the longitudinal section intersects the latitude 9°S for the sections NS2 - NS6 and at the distance 440 km from the point 5°S, 129°E for the triangular sections az180 - az80. Position of longitudinal section is shown in Figure 3. The dip of the plane is 60°. The coordinates of transformed focal mechanisns were rotated by the strike and dip of the southern WBZ, transformed coordinates were chosen equivalent to that of plane of longitudinal section. The Cartesian coordinates are oriented as follows: x-axis toward the north, y-axis toward the east and z-axis down, whereas the transformed coordinates are oriented as follows: x'-axis against the direction of subduction, y'-axis along the strike of the plane of the WBZ and z'-axis perpendicular to the WBZ. The dip of x'-axis is 60° for all focal mechanisms, but the strike changes along the plane of the WBZ according to the bending of this plane. For the focal mechanisms belonging to the north-south sections and section az180 the strike is 270°. With the decreasing strike of triangular sections, the strike of transformed focal coordinates decreases, too: strike for the section az170 is 260°, strike for the section az160 is 250° etc.

The longitudinal section along the Seram trough was constructed projecting the earthquake foci to the plane of the northern WBZ (Figure 28). The surface trace of the longitudinal section intersects the latitude 2°S for the sections NS1 - NS9 and at the distance 370 km from the point 5°S, 129°E for the triangular sections az40 - az70. Position of the longitudinal section is shown in Figure 3. The dip of the approximating plane is 50°. The focal mechanisms were not transformed to plane defined by parameters characterizing the WBZ because just a few focal mechanisms are found in the intermediate-depth and deep part of the WBZ. For the shallow part of the WBZ the orientation of the segment does not fit the orientation of the longitudinal section.

The beachball diagrams were depicted into EHB hypocenters in longitudinal sections (Appendix 1 and Figure 28).

By means of the method described above, it is possible: (1) to define the Wadati-Benioff zone and to determine its geometrical parameters – dip, depth range, and thickness; to visualize non-uniform distribution of seismic activity in the WBZ and (2) at overriding plate, to interpret the earthquake distribution by comparison with surface morphology and tectonics (e.g. volcanoes, fracture zones) and to find the parameters and tectonic function of respective structures.

Special attention was paid to mainshock-aftershock sequences. A mainshock-aftershock sequence was defined as a sequence of at least 15 events, including mainshock, which took place in a short time interval of several months at maximum. The analysis of spatial distribution of the earthquake foci in mainshock-aftershock sequences points to a quasi-planar distribution of earthquakes, manifesting the occurence of the aftershocks along faults. This general feature of mainshock-aftershock sequences enables to calculate the geometrical parameters of a respective approximating plane (its strike and dip).

The least-squares method was used to search for an optimum plane approximating the foci of a mainshock-aftershock sequence. The optimum solution is defined by minimization of the misfit function and is found by a grid search with 0.5° step in both strike and dip. The stability of optimum solution for individual sequences has been tested by its comparison with the best 10% of all solutions for each sequence. The results were usually calculated for two datasets: the first one includes all EHB events and the second one includes only EHB events characterized as DEQ. Negligible differences in strike and dip for both sets points to a high quality of the EHB dataset as a whole. Detailed description of the method of approximation is given in Špičák et al. (2007b).

The spatial distribution of earthquake foci is analysed simultaneously with available focal mechanisms. The HCMT solutions were assigned to EHB events and depicted to the sections (Figures 4 – 28, Appendix 1). The HCMT solutions are captioned by HCMTS code in Figures 4 – 28 and Appendix 1; the code represents the date of the event occurrence.

4. Observation and interpretation

The Banda Arc belongs to the most seismically active areas in the world. The EHB catalogue involves almost 3000 events selected from the Banda Sea region, bounded by latitudes 2°S and 10°S and by longitudes 124°E and 135°E during the 41 years period (1964 - 2004); for over 500 of them, focal mechanisms are available. There are no subperiods of marked decrease or increase in seismic activity during the 41 years period of observation.

Epicentral map of earthquakes in the Banda Sea region is shown in Figure 3. Intense seismicity can be observed namely between the Timor-Tanimbar-Aru and Seram troughs and the volcanic arc. Intermediate and deep earthquakes are distributed beneath the Banda Sea. The Banda Arc is characterized by a Wadati-Benioff zone (WBZ) bent by about 180°. The WBZ dips inward from the south, east, and north to depths down to 500 km beneath the Banda Sea.

The Banda Sea region is surrounded by seismically active zones of Sulawesi in the northwest, the Sorong Fault zone in the north and New Guinea in the northeast and east (Figure 3). The adjacent seismicity is shallow and belongs to collision zones of microplates and plates. In the southeast and south of 9°S, no earthquakes occur within the Indo-Australian plate. West of 126°E, the Banda Arc merges into the Sunda Arc where the oceanic lithosphere of the Australian plate subducts beneath SE Asia along the Java trench. The continuity is probably only apparent because the arcs are stratigraphically and structurally very different (Audley-Charles, 1981). The adjacent seismicity is depicted in gray color in the sections (Figures 3 – 27, and 29), but it is not analyzed in this thesis as it is situated outside the investigated area. Nevertheless, the influence of adjacent seismically active structures on kinematics of the investigated region has to be taken into account.

The first step of the work was to separate seismic events that belong to the Wadati-Benioff zone from those that are situated in the overriding plates on the basis of an analysis of the spatial distribution of earthquake foci. The events were separated by displaying the hypocenters of events in vertical sections (Figures 4 - 27) with respect to the significant morphological structures in the region: the Timor-Tanimbar-Aru and Seram troughs, the Weber deep and the inner volcanic arc. When the separation is not clear in one section, the neighboring vertical sections and available fault plane solutions were checked.

In the eastern bent part of the arc around 4.5°S, 131.5°E, no earthquake is observed in the epicentral map (Figure 3). To the south and southwest, the seismicity is more intense than to the north and northwest from this area. Based on a preliminary analysis of the epicentral map, the Banda Arc was separated into two parts - the southern and northern limbs (Figure 29). The boundary between these two probably different subduction zones was situated along the Tarera-Aiduna fault zone (TAFZ). The southern limb is delimitated from the Timor island to TAFZ and the northern limb of the Banda Arc is delimitated from TAFZ to the Buru island.

The description of earthquake occurrence will proceed in the following manner: from the west to the east and southeast for the southern limb and from the southeast to the northwest and west for the northern limb of the Banda Arc, i.e. counterclockwise.

4.1 Vertical sections and morphology of the Wadati-Benioff zone

4.1.1 Southern subduction

The southern subduction zone we named Banda subduction. The earthquake distribution expressed in vertical sections points to the existence of a well-defined Wadati-Benioff zone of the Banda subduction. The western termination of the relatively shallow WBZ is at longitude 126.5°E (section NS2, Figure 5) at the eastern end of the Timor island. The WBZ can be traced along the axis of the Weber deep, it is bent to the north and terminates at 131°E (section az80, Figure 23). The laterally continuous seismicity of the southern WBZ is clearly visible in the epicentral map (Figure 3). The southern WBZ is delimitated in sections NS2 - NS6 and az180 - az80 (Figures 5 – 9 and 13 - 23). The two sets of sections overlap in sections NS6 and az180 (Figures 9 and 13); except these two sections, each event of the southern limb is depicted just in one of the 16 sections.

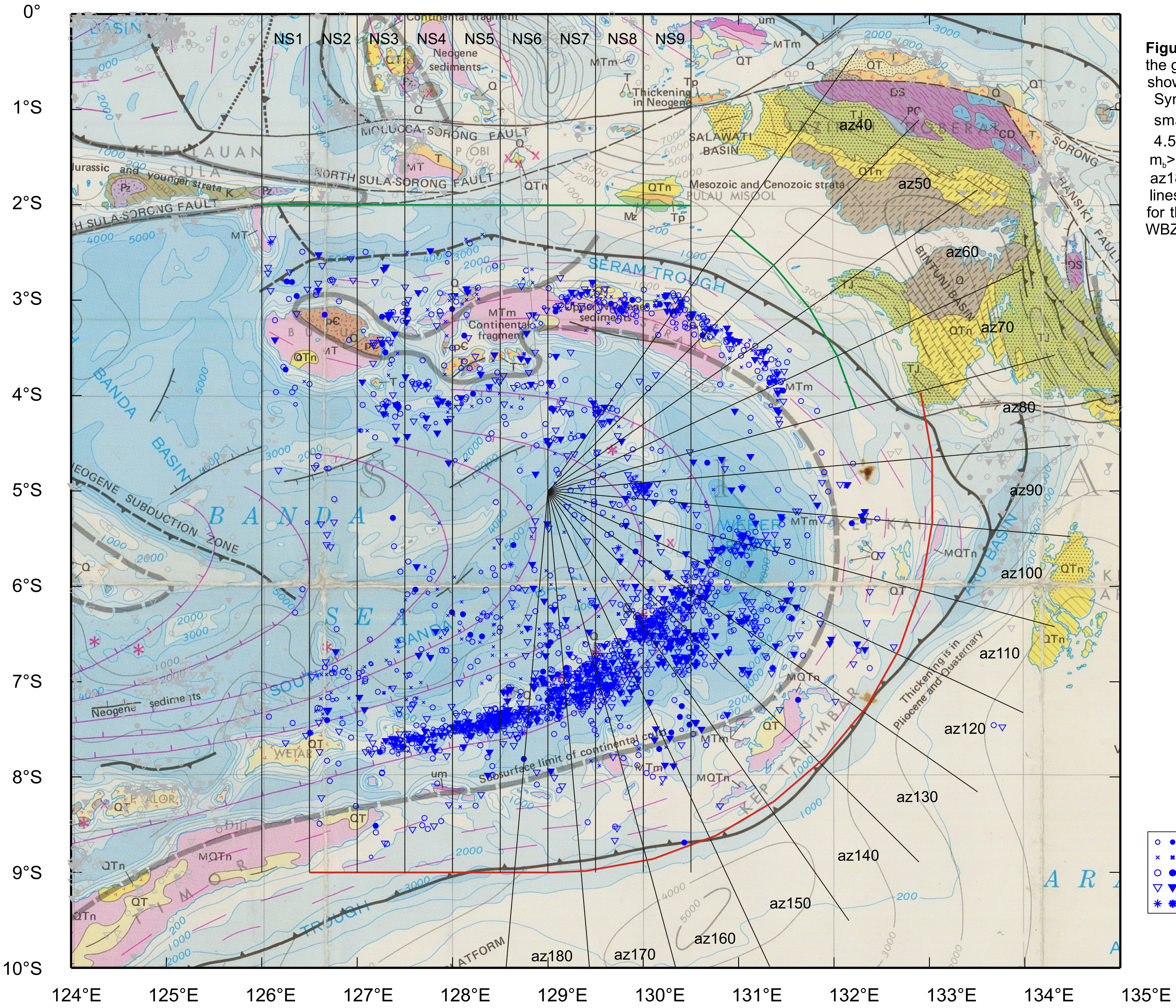

Figure 3. Epicentral map of the Banda Sea region with the geological map by Hamilton (1978) in the background shows the distribution of earthquakes in the Banda Arc. Symbols of earthquakes with EHB magnitude m_b: small circles, $m_b \leq 4$, crosses, $4 < m_b \leq 4.5$, circles, $4.5 < m_b \leq 5$, inverted triangles, $5 < m_b \leq 6$, asterisks, $m_b > 6$. Boundaries of sections NS1 - NS9 and az40 - az180 are denoted by thin black lines, the reference lines for longitudinal sections are denoted by red line for the southern WBZ and by green line for the northern WBZ.

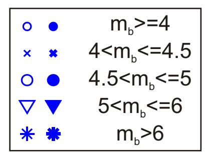

Beneath the Timor island, no seismicity is observed (section NS1, Figure 4, and Figure 10a in Špičák et al., 2007a). The seismic activity gradually appears eastward of the Timor island (section NS2, Figure 5). Shallow events of the southern WBZ are distributed between the volcanic arc and fore-arc ridge (Figure 3). Along the Timor-Tanimbar-Aru troughs there is no seismicity. It appears that the inclined slab does not start along the trough, being shifted toward the volcanic arc, similarly to the slab in the area of the Java trench (Hanuš et al., 1996).

Hypocenters show that the dip of the WBZ decreases from 70° (section NS2, Figure 5) to 40° (section az80, Figure 23). The depth of the slab penetration, manifested by the deepest earthquakes in individual sections, varies considerably from 500 km in the west to 200 km in the east and southeast (Appendix 1). The thickness of the WBZ, measured perpendicularly to the direction of subduction, varies between 20 km and 80 km in the upper part and between 40 km and 80 km in the lower part of the downgoing slab. The distribution of earthquake foci is nonuniform within the WBZ (Appendix 1). There can be observed domains of intense seismicity as well as zones of low seismicity or aseismic gaps without any EHB event.

At the western shallow part of the WBZ (down to 100 km depth) there is an absence of earthquakes from 126.5°E to about 130°E (sections NS2 - NS6, az180 and az170; Figures 5 – 9, 13 and 14). Only few events in the depth range 0 - 100 km are present in sections NS2 - NS6 between 8°S and 9°S, and between the distance of 250 and 400 km along x-axis in sections az180 - az170.

Beneath this shallow seismicity a peculiar intermediate-depth domain of the highest seismicity and of the largest concentration of CMT mechanisms of the Banda Arc occurs. The domain, starting at 127°E between 100 km and 220 km depth (section NS3, Figure 6), is unusually vertical and narrow, which is not consistent with the inclination of the WBZ,. At 129°E (sections NS6 and az180, Figures 9 and 13), where the intensity of the domain is the highest, the width of the domain increases (section az180, Figure 13), occurs at greater depths (Appendix 1) and is divided into two parts. The deeper one is distinguishable from 129.5°E (section az170, Figure 14) between 120 km and 220 km depth and terminates at 4°S (section az80, Figure 23) in shallow depths of 50 – 100 km. From 130°E (section az120, Figure 19), both parts of the domain are clearly separated and are situated in smaller depths. The shallower one is joined to shallow earthquakes of the WBZ and from about 131°E (section az140, Figure 17) it lies in depths between 0 km and 150 km. From section az110 to the north, a decrease in seismic activity can be observed and this part of the domain probably terminates there. More to the southeast of the domain, few shallow events can be found, closer to the trench between sections az110 - az80 (Figures 20 - 23) separated by a gap.

Focal mechanisms of events within the intermediate-depth domain displayed in the standard map view are of both normal and reverse type. Predominant are events with focal mechanism of reverse type. Transformation of focal mechanisms with respect to the plane defined by the WBZ (see longitudinal section in Appendix 1) revealed that the focal mechanisms of reverse type were transformed to mechanisms of normal type in the view of the WBZ plane. Focal mechanisms with the similar orientation of nodal planes can be found within the whole domain, but the accumulations of events within the domain include focal mechanisms of differently oriented nodal planes and different magnitudes. Nonuniform orientation of nodal planes and stress axes indicate that tectonic regime of the domain is not easily interpretable. The domain requires a detailed study and analysis of focal mechanisms.

One of the prominent features of the southern WBZ is the existence of aseismic zones within the subducted plate with extreme variability of their upper and lower limits (Appendix 1). The deepest earthquakes are separated from the intermediate-depth domain by an aseismic zone that is 30 km to 140 km wide. The depth of the upper limit varies laterally from 160 km to 220 km and the lower limit varies from 200 km to 300 km.

The southern slab is subducted at depths 70 - 100 km beneath the volcanic arc (Table 2). The existence of calc-alkaline volcanism is a general feature of WBZ in those regions where the process of subduction reached a certain depth. This depth is governed by the local state conditions in the downgoing slab. The partial melting of the slab can be considered as the primary source of magma and influences the geochemical composition of magma. At the same time, the decreased viscosity due to the partial melting of the lithospheric material would exclude the accumulation of stress as the necessary condition for generation of earthquakes (e.g. Špičák et al., 2003). The intermediate-depth aseismic gap is less distinct than the deeper aseismic zone and is visible only in the longitudinal section (Appendix 1). The aseismic gap is hardly detectable in vertical sections (Figures 4 – 9 and 13 – 23). This intermediate-depth aseismic gap runs continuously through the whole WBZ. The depth and thickness of aseismic gap vary laterally. In the northeast part of the WBZ the aseismic gap is less wide than in the west.

A detailed description of parameters of the southern WBZ is given in Table 2.

4.1.2 Northern subduction

The northern subduction zone we named Seram subduction after the Seram trough along which the slab sinks beneath the northern limb of the Banda Arc. The principal difference between the southern and northern WBZ is that the northern WBZ has much lower seismic activity and is less curved laterally compared to the southern WBZ. The northern WBZ is delimitated between 126°E to 131°E in sections NS1 - NS9 and az40 - az70 (Figures 4 – 12 and 24 – 27) and is just moderately bent to southeast. The two sets of sections overlap in a small area in sections NS7 - NS9 and az40 - az70 (Figures 10 – 12 and 24 - 27), but only a few events are situated in more than just in one section.

The northern WBZ dips at about 35° to southwest and reaches the depth of only 200 km in the east; in the west the dip increases to 60° and the depth is over 500 km. The width varies between 50 km and 80 km for the upper part, and between 30 km and 90 km for the lower part of the WBZ. The seismicity is not continuous with depth (Figure 28); the WBZ does not appear like representing a single uninterrupted plate-like body.

The most dominant phenomenon of the northern WBZ is about 300 km long shallow segment along the Seram trough from 131°E (section az70, Figure 27) along the northern margin of the Seram island (sections az60 - az40 and NS9 - NS7; Figures 24 – 26 and 10 - 12). The earthquake foci are concentrated in a segment that does not remind an onset of a subducting plate. The width of the segment varies between

Table 2. Attributes of vertical sections					southern Banda subduction									northern Seram subduction								
										parameters of WBZ									parameters of WBZ			
	section	Figure	number of events in the Banda Sea region dataset	number of FM	* T [km]	* W [km]	* C [km]	* position of volcano [km]	depth of WBZ beneath the volcano [km]	dip [°]	maximum depth [km]	width of upper/ lower part [km]	depth range of asesimic gap [km]	* T [km]	* W [km]	* C [km]	* position of volcano [km]	depth of WBZ beneath the volcano [km]	dip [°]	maximum depth [km]	width of upper/ lower part [km]	depth range of asesimic gap [km]
rectangle sections	NS1	4	45	5			930			-	-	-	-	240, 300		360			-	90	-	-
	NS2	5	70	7			920	730	-	70	470	20/40	220-270	280		370			-	440	80/-	90-390
	NS3	6	130	29			910			70	440	20/60	220-270	280		390			60	430	80/30	100-230 200-400
	NS4	7	166	33			900			65	420	40/70	200-300	280		400			60	310	60/50	90-200
	NS5	8	240	39	990	880	900			65	410	60/60	210-270	260		420			50	410	70/70	220-280
	NS6	9	242	50	990	850	890	770	70	60	350	60/80	-	260		420			45	350	60/90	190-230
	NS7	10	313	58										270	390	360			40	300	50/80	-
	NS8	11	357	48										280	410	360	500	150	-	230	60/90	80-150
	NS9	12	320	74										290	440	380			-	150	60/-	-
triangular sections	az180	13	147	34	430	270	330	220	110	60	300	50/80	-									
	az170	14	165	26	440	270	330			60	250	50/70	210-220									
	az160	15	168	26	440	260	320	200	80	55	280	70/40	180-200									
	az150	16	99	26	460	240	330	180	80	55	200	70/80	180-200									
	az140	17	167	36	450	230	340			55	210	80/50	170-200									
	az130	18	117	27	450	230	360			55	220	70/-	190-220									
	az120	19	103	20	450	240	360			50	200	80/-	160-200									
	az110	20	49	12	480	230	360	150	-	-	130	70/-	-									
	az100	21	75	19	510	230	340			-	130	60/-	-									
	az90	22	121	23	500, 540	210	330			-	110	50/-	-									
	az80	23	46	11	450, 560	200	310			-	120	50/-	-									
	az40	24	59	8										330	180	230			-	380	60/50	-
	az50	25	36	7										340	180	240			-	400	60/40	-
	az60	26	60	8										370	180	270			-	70	70/-	-
	az70	27	31	5										400	180	290			-	170	50/20	-

* numbers indicate the distances along the vertical sections (x-axis)

50 km and 80 km; the segment dips almost vertically with a moderate inclination to the south. The deepest earthquakes in this segment are only about 80 km deep. The inclination of the intermediate-depth and deep levels of the WBZ differs from the dip of the shallow segment. The focal mechanisms in the segment are uniform and of reverse type (Figure 28).

The seismicity that is situated along the Seram trough (sections NS1 - NS6, Figures 4 - 9) belongs to the WBZ. At 128.5°E (sections NS5 and NS6, Figures 8 and 9) a small gap can be found and to the west (126°E – 129°E) the segment probably continues but cannot be distinguished from overall shallow earthquakes. To the west, shallow earthquakes are less concentrated. Focal mechanisms in this part of the northern limb (sections NS1 - NS5, Figures 4 - 8) are of reverse and strike-slip type.

The deepest earthquakes in section NS2 (Figure 5) do not fit geometrically the distribution of earthquakes in section NS1 or NS3 (Figures 4 and 6). The deepest earthquakes in sections NS1 and NS2 between the depth of 300 km and 500 km probably belong to Sulawesi seismicity (Das, 2004), therefore these earthquakes are not analyzed in this thesis. The delimitation of the deepest earthquakes is ambiguous especially beneath the longitudes 128°E – 130°E (sections NS5 - NS8, Figures 8 - 11). There the collision of the southern and northern subducting plates probably occurs at the depth range of 200 – 400 km. It is not easy to decide to which plate these earthquakes belong. But it looks as if the northern plate penetrates deeper than the southern plate which collides with it. The focal mechanisms of reverse type with different orientation of nodal planes are typical for the collision of these two subducting plates.

In the intermediate-depth and deep levels of the WBZ, aseismic zones can be found in comparison with the continuously active southern subduction (see the longitudinal section, Figure 28). The concentration of earthquakes in the depth range of 100 – 200 km can be observed in sections NS5 - NS7 (Figures 8 – 10), in the longitudinal section it is at the distances of 140 – 300 km down-dip the WBZ and at the distances of 220 – 360 km along the longitudinal section. The largest concentration of earthquakes is in the depth range of 200 – 300 km (sections NS3 – NS9, Figures 6 - 12), in the longitudinal section it is at the distances of 300 - 450 km down-dip the

WBZ and at the distances of 100 – 780 km along the longitudinal section (Figure 28). The deepest earthquakes (300 - 500 km deep, sections NS3 - NS7; Figures 6 - 10) in the longitudinal section at the distances of 450 - 650 km down-dip the WBZ are concentrated at the distances of 140 – 400 km along the longitudinal section (Figure 28). The focal mechanisms of intermediate-depth and deep earthquakes displayed in the standard map view are of both reverse and normal type with differently oriented nodal planes.

The depth of the northern slab beneath the volcanic arc is about 150 km (section NS8, Figure 11). Banda Api is the only known recently active volcano of the Seram subduction. The existence of active volcanoes along the western part of the northern limb of the arc is not clear.

A detailed description of the parameters of the northern WBZ is given in Table 2.

After the above analysis, no other intermediate-depth and deep earthquakes remained in the Banda Sea dataset. All events of that kind in the dataset were included into the southern WBZ (coloured light blue in Figure 29) or northern WBZ (coloured red in Figure 29), respectively. Sometimes the separation was not unambiguous, especially at the deep collision zone. The usage of neighboring sections was in this case ineffective and focal mechanisms were not available.

4.2 Seismicity of the overriding plate

About 10 % of earthquakes of the Banda Sea region dataset (305 of 2961 EHB events) belong to the overriding plate. The earthquakes are situated beneath the Banda Sea in the back-arc region at the depth range 0 - 85 km. The distribution of earthquake foci in the overriding plate was confronted with the position of volcanoes and fracture zones. An investigation into the distribution of earthquake foci above the subduction zones revealed the existence of clusters of earthquakes below active calk-alkaline volcanoes. These clusters, denoted as seismically active columns (SAC), may contribute to the solution of the problem of source region and mode of transportation of primary magmas for active volcanoes at convergent plate margins (e.g. Špičák et al., 2004).

Besides the volcano-related seismicity, two mainshock-aftershock sequences were found within the overriding plate. The distribution of earthquake foci of mainshock-aftershock sequences or clusters of earthquakes can overlap with the position of fracture zones in the map view. A plane approximation of the distribution of foci in the mainshock-aftershock sequences was used to analyze the internal tectonic structure of fracture zones (Špičák et al., 2007b).

The following description of the seismicity of the overriding plate will proceed in the same sense as in the previous sections: from the west to the east, and then to the north and to the west along the volcanic arc, and finally beneath the Banda Sea.

North of the Wetar island, along the longitude 7.5°S and between latitudes 126°E and 128.5°E (sections NS1 - NS5, Figures 4 - 8), 27 events were observed along the Wetar thrust (coloured dark blue in Figure 29). The 8 westernmost ones of them in sections NS1 - NS3 probably belong to the Wetar thrust, as focal mechanism C052191A indicates. 19 events in sections NS3 - NS5 probably lay beneath the volcanic arc. They can belong to the Wetar thrust, too or they can be associated with submarine volcanic seamounts and reflect their active plumbing system.

Eastwards, the volcanic arc is curved to the northeast and the volcanoes Damar (or Wurlali, 7.1°S, 128.7°E), Teon (6.9°S, 129.1°E) and Nila (6.7°S, 129.5°E) have SACs (coloured orange in Figure 29) with a mainshock-aftershock sequence at Damar. The SACs of Damar and Teon overlap and contain 32 events with 14 focal mechanisms. The SAC lies beneath the Damar and between Damar and Teon in the depth range 0 - 50 km in sections NS6 and az180 (Figures 9 and 13). The majority of focal mechanisms are of strike-slip and 5 of reverse type. 17 events of 32 (5 with focal mechanism) belong to the sequence of November 1998. The best solution of the approximation of the sequence is the plane with strike 45° and dip 60° for EHB events characterized by DEQ tag. The approximation of the sequence for all EHB events gave different solution – the plane with strike 80° and dip 70°.

The volcano Nila (sections az170 and az160, Figures 14 and 15) has a SAC of 9 events from May 1968 to April 1976, without any focal mechanism available. The SAC is situated beneath the volcano at the depth range 0 - 40 km. The May 4, 1968 event with magnitude m_b=5.7 was accompanied by a volcanic eruption.

The largest cluster of 48 events (3 with focal mechanism) with a mainshock-aftershock sequence of 37 events occurred at longitude 130°E and latitude 5°S (sections az90, NS8 and NS9; Figures 22, 11 and 12; coloured pink in Figure 29). The cluster is not situated at the volcanic line but is probably associated with the tectonic activity of the Tarera-Aiduna fault zone inside the Banda Sea. The cluster is situated beneath the western termination of TAFZ as is evident in the morphological map (Figure 2). The maximum depth of an earthquake in the cluster is 70 km. Two focal mechanisms are of strike-slip type and one is reverse. The sequence from December 1974 to March 1975 includes two mainshocks with magnitude m_b=6; no event with focal mechanism is available in the sequence. The best solution of the approximation of the mainshock-aftershock sequence is the plane with strike 70° and dip 70° for EHB events characterized by DEQ tag. The best solution for all EHB events is the plane with strike 90° and dip 75°.

The SAC of the Banda Api volcano (4.5°S, 129.9°E, Figure 11; coloured orange in Figure 29) consists of 30 events in the depth range 0 - 85 km which are aligned in the NNW-SSE direction in the NW base of the volcano. The faulting indicated by 5 focal mechanisms is reverse. One of the nodal planes of each focal mechanism is parallel to the direction of earthquake distribution.

Remaining 41 events in the southeastern part of the Banda Sea can belong to submarine volcanic seamounts if their position could correlate with the line of the volcanic arc. However, the distribution of events coloured green in Figure 29 does not correlate with the volcanic line; it appears that they show a tendency to accumulate in linear zones, parallel to ENE-WSW trending faults mapped by Hinschberger et al. (2003, 2005). Their focal mechanisms are of strike-slip type and one of the nodal planes has the direction of these faults, parallel to the Timor-Tanimbar-Aru trench.

The shallow seismicity along the northern limb of the Banda Arc has a character different from the overall seismicity in the Banda Sea region. Ninety-nine events (21 with focal mechanisms) were selected in the area south of the Buru and Seram islands between longitudes 127°E and 129.5°E (coloured yellow in Figure 29). This group of earthquakes includes 2 small sequences no longer than a couple of days: in February 1998 (10 events) and in August 2000 (9 events). The maximum depth of earthquakes is 85 km. The sea floor in this part of the Banda Sea has a rugged morphology; the occurrence of seamounts is disputable. Hence the origin of earthquakes associated with submarine magmatic activity cannot be excluded. As the depth range correlates with the thickness of the lithosphere, the seismicity can be induced by the motion on microplate boundaries as well.

Less than 20 earthquakes with maximum magnitude m_b=5.3, which is less than 1 % of the whole Banda Sea region dataset could not be correlated with any tectonic structure (colored black in Figure 29). Their occurrence is isolated and no focal mechanism is available. They are probably associated with zones of weakness or deformation zones in the back-arc region.

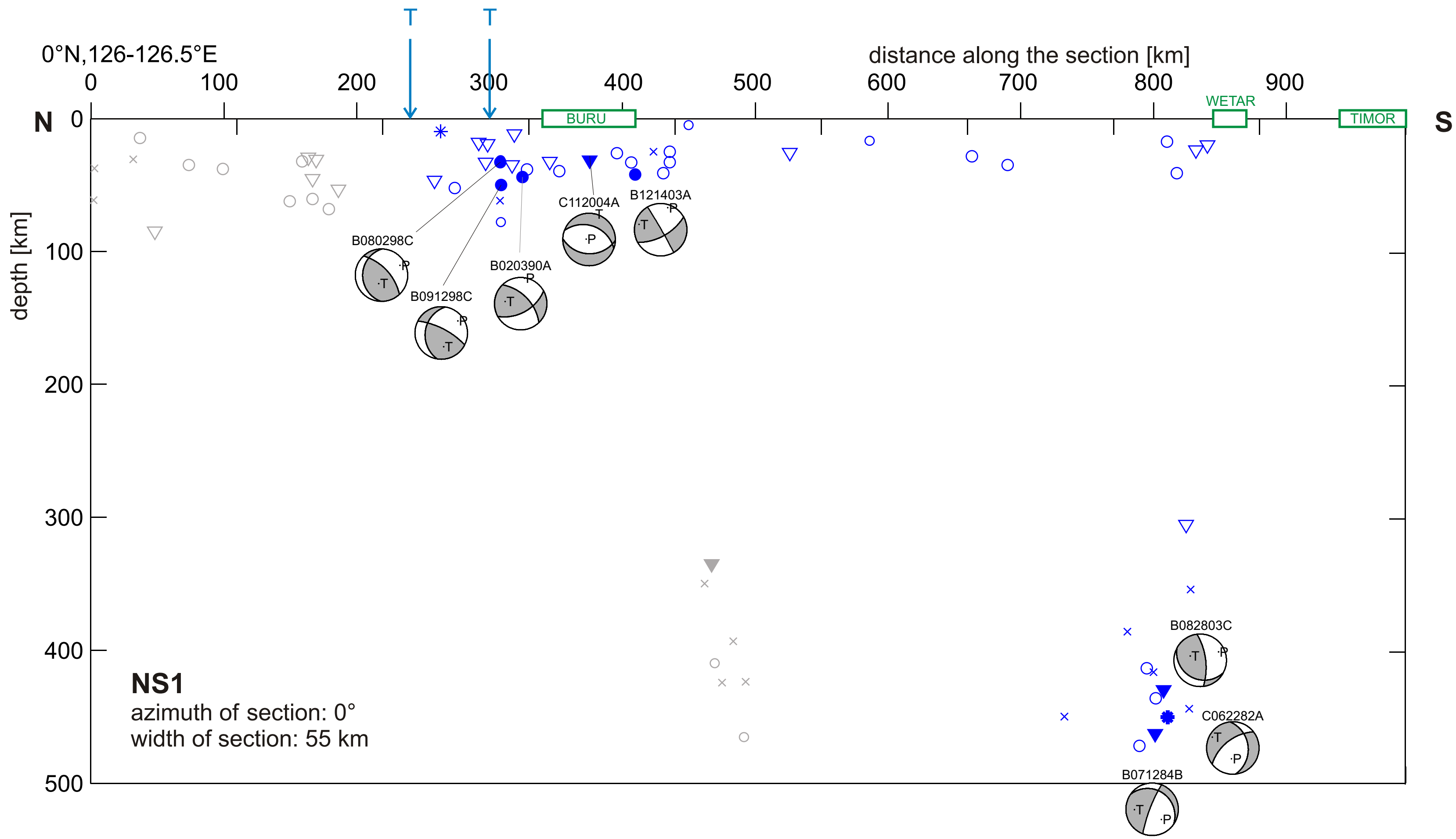

Figure 4. Vertical section NS1. For the section position and symbols of earthquakes see Figure 3. Orange trianges indicate the position of active volcanoes, green rectangles indicate the position of island. T, axis of the Timor-Tanimbar-Aru and Seram trough, W, Weber deep, C, limit of continental crust of the Australian plate (Hamilton, 1978, see Figure 3).

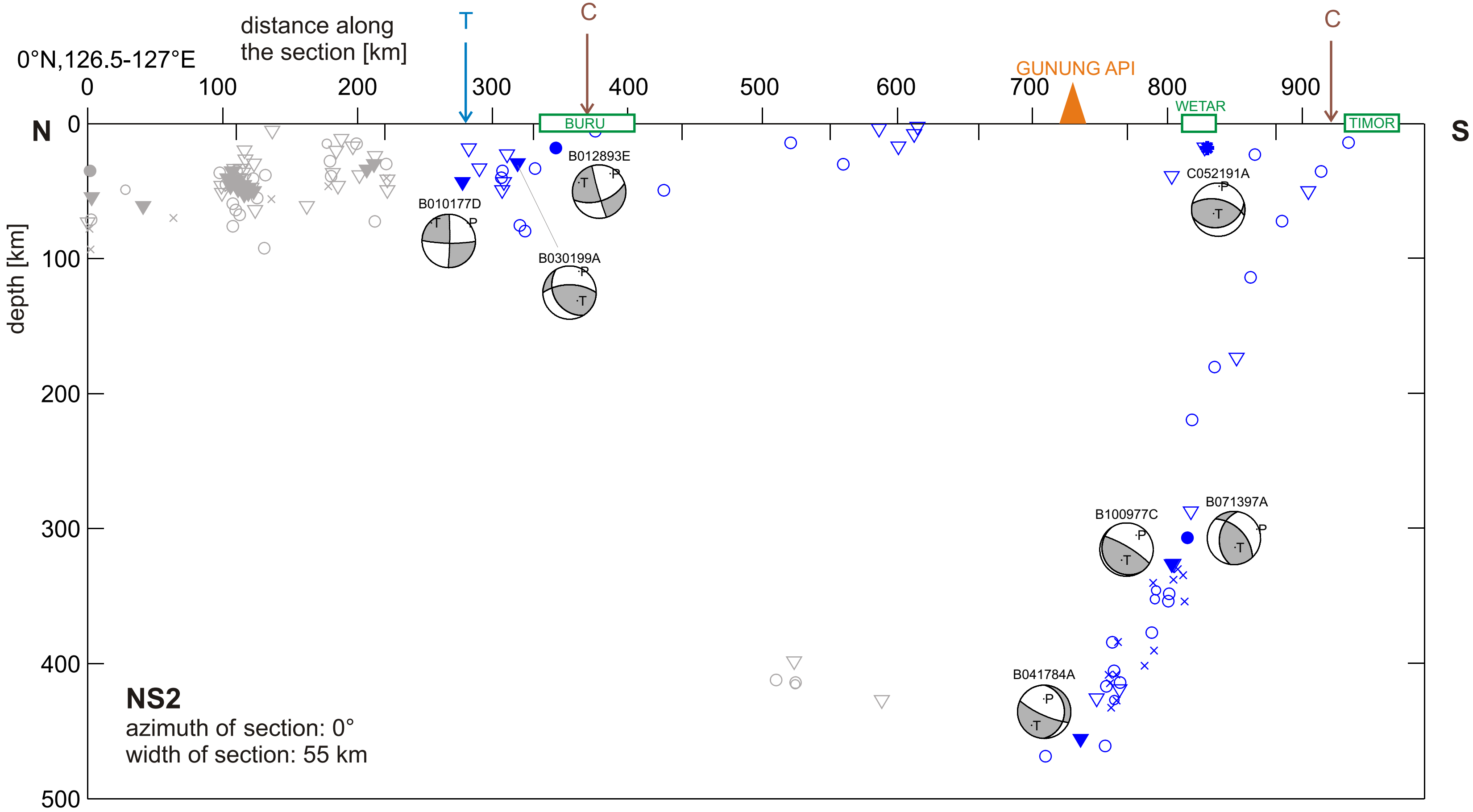

Figure 5. Vertical section NS2. For the section position and symbols of earthquakes see Figure 3, for other symbols see Figure 4.

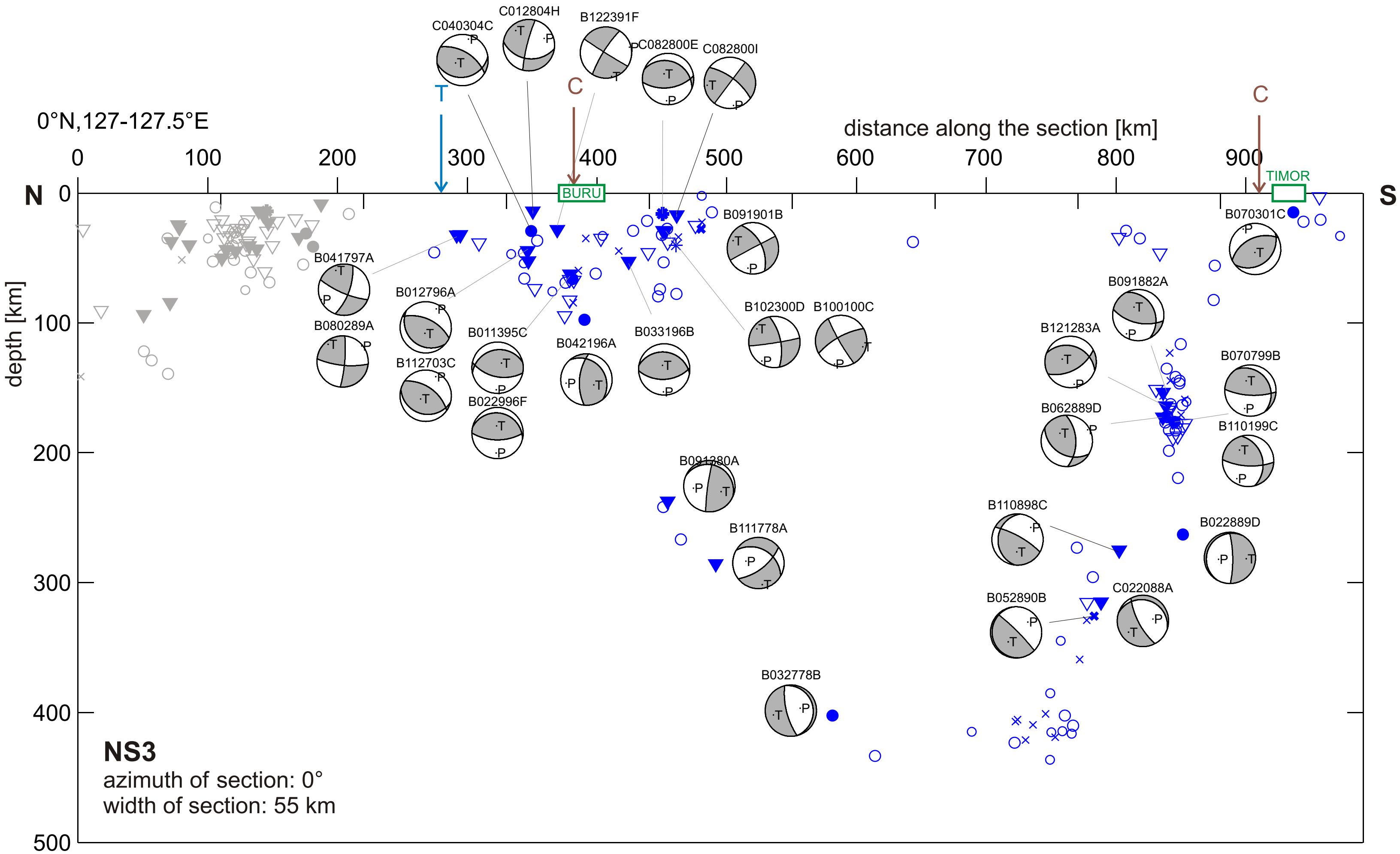

Figure 6. Vertical section NS3.For the section position and symbols of earthquakes see Figure 3, for other symbols see Figure 4.

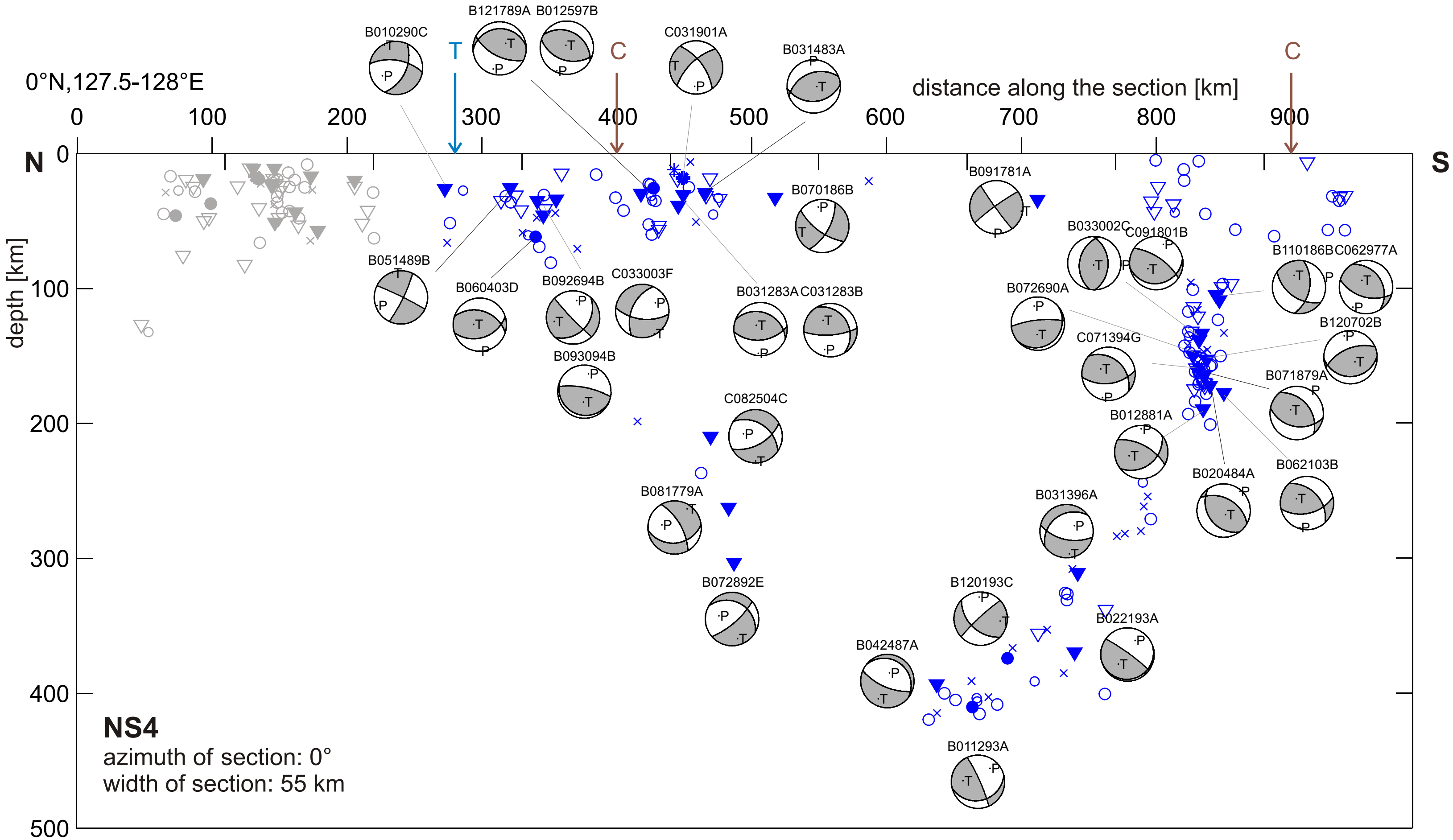

Figure 7. vertical section NS4.For the section position and symbols of earthquakes see Figure 3, for other symbols see Figure 4.

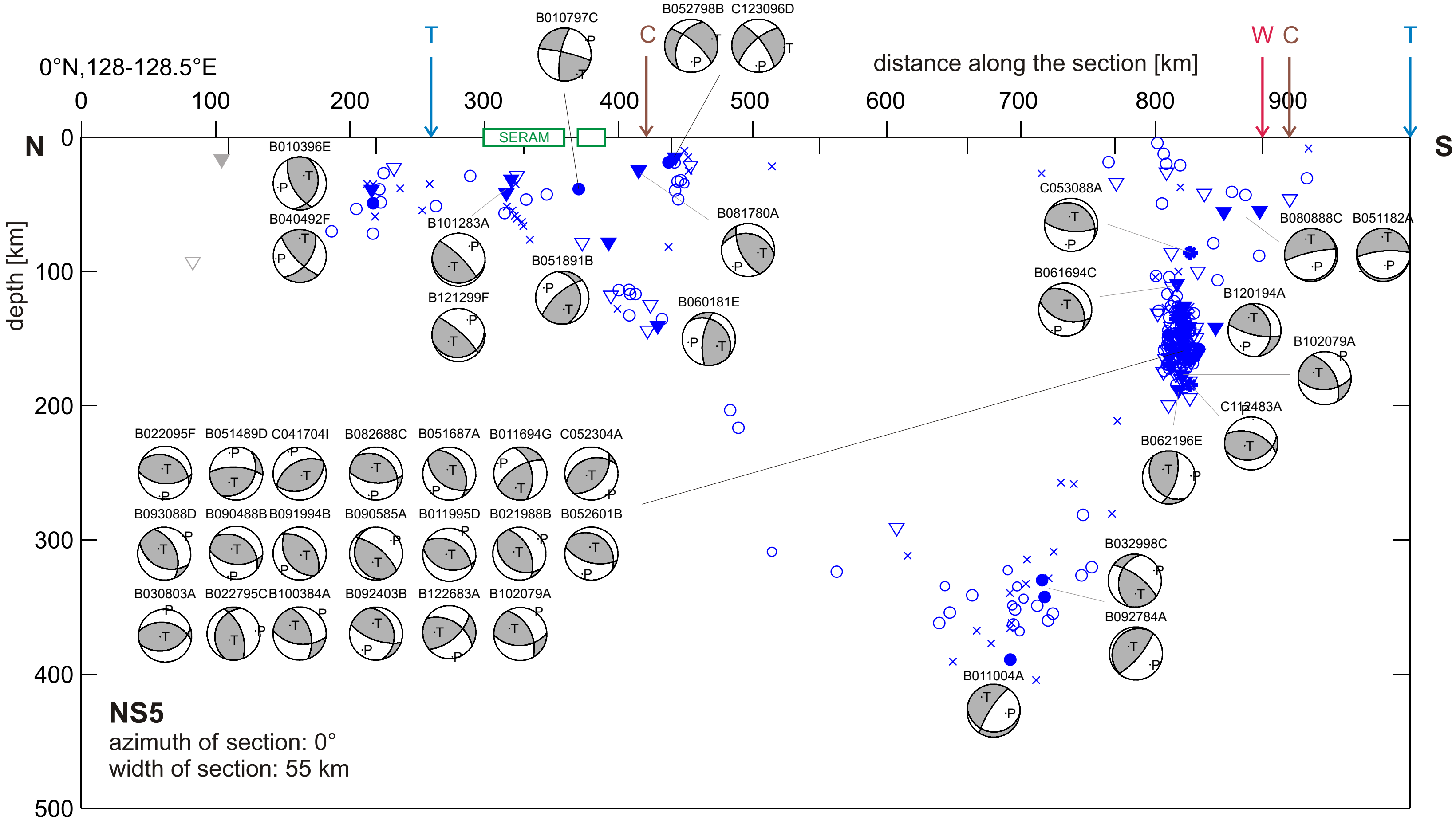

Figure 8. Vertical section NS5.For the section position and symbols of earthquakes see Figure 3, for other symbols see Figure 4.

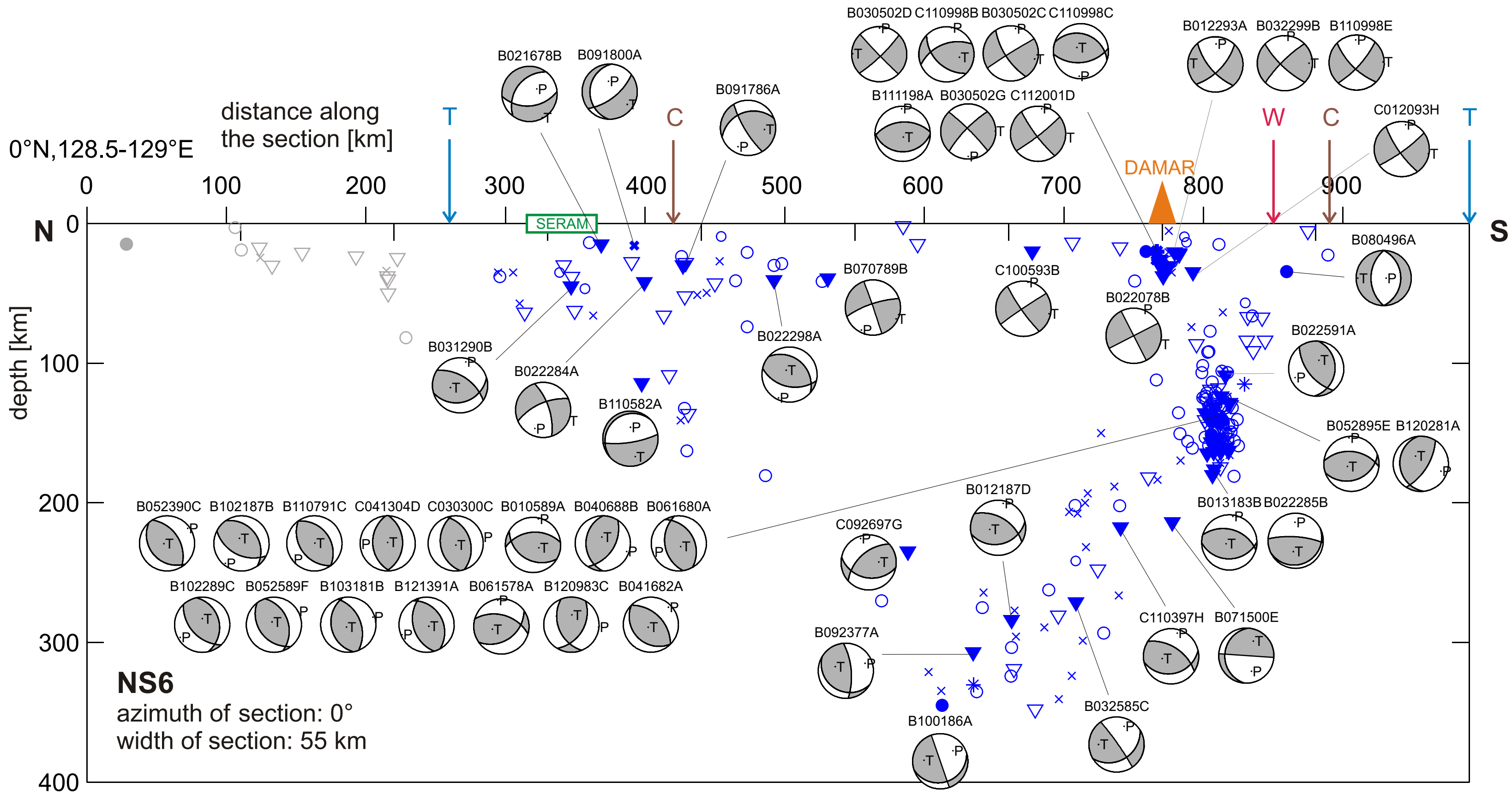

Figure 9. Vertical section NS6. For the section position and symbols of earthquakes see Figure 3, for other symbols see Figure 4.

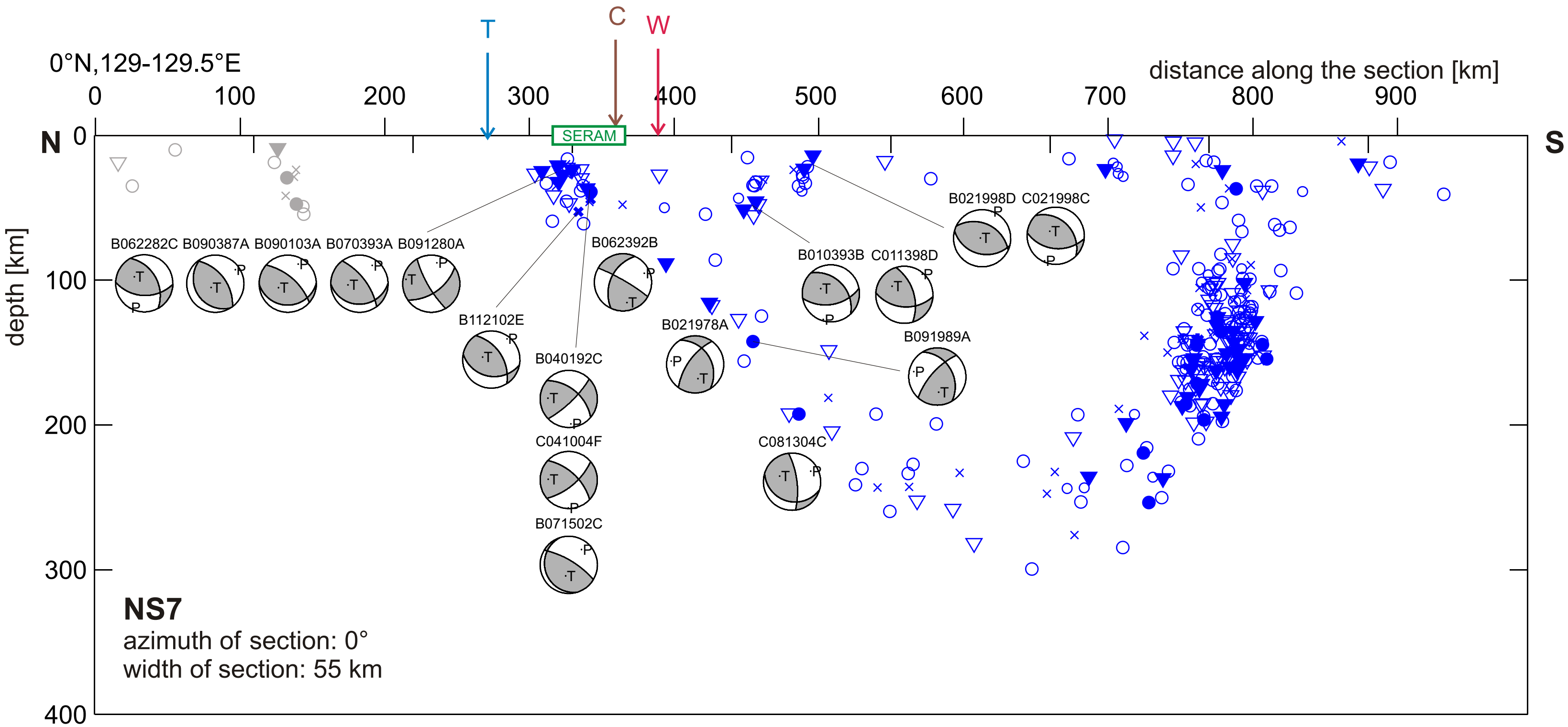

Figure 10. Vertical section NS7. For the section position and symbols of earthquakes see Figure 3, for other symbols see Figure 4.

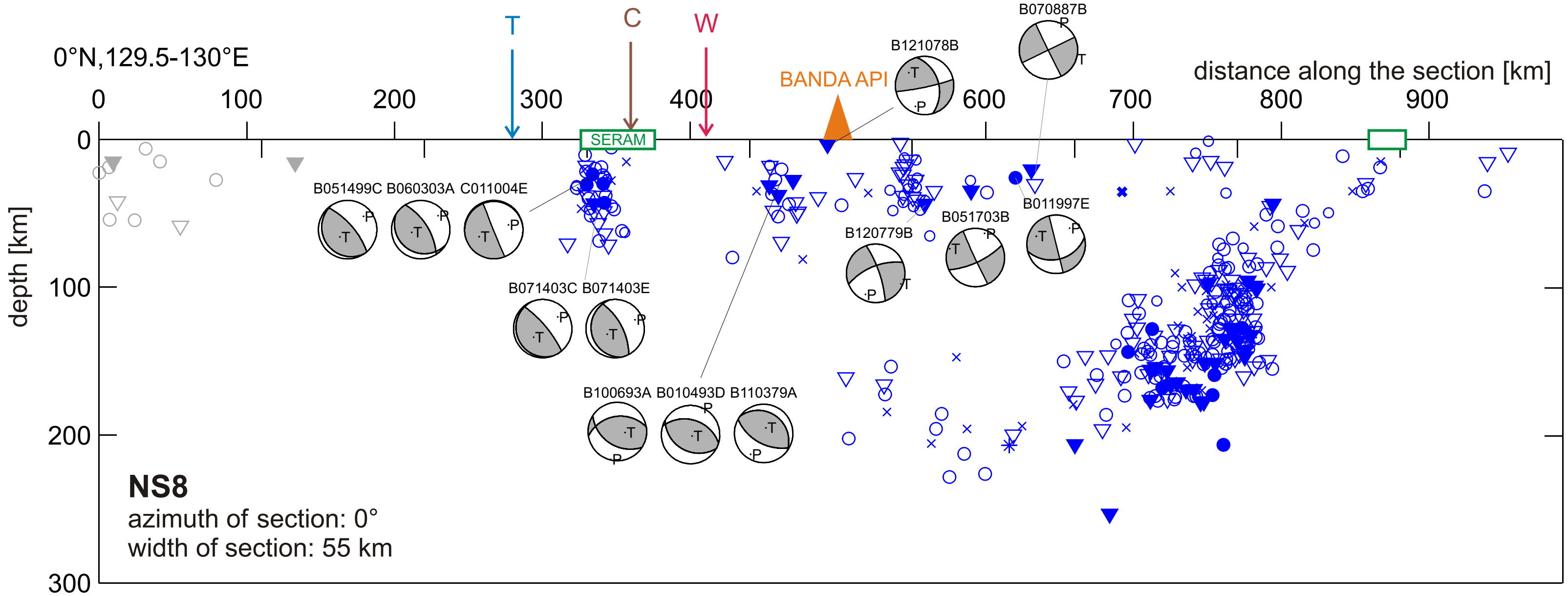

Figure 11. Vertical section NS8. For the section position and symbols of earthquakes see Figure 3, for other symbols see Figure 4.

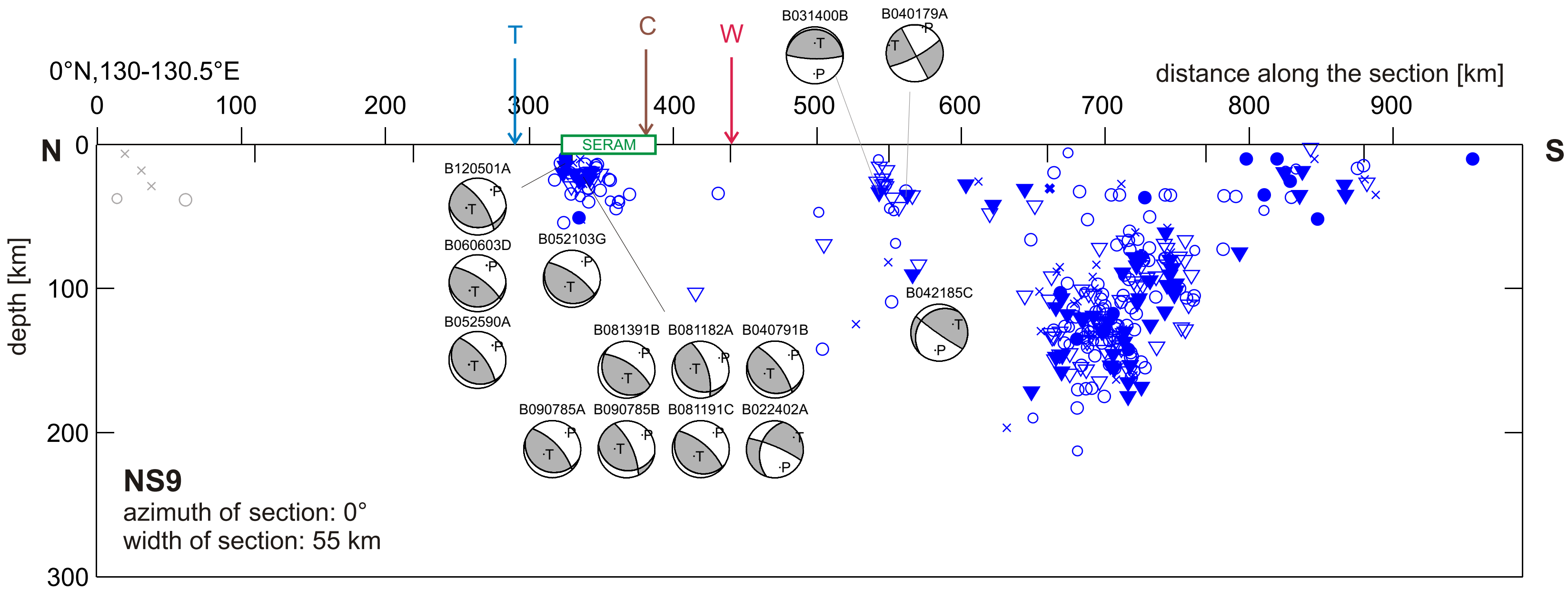

Figure 12. Vertical section NS9. For the section position and symbols of earthquakes see Figure 3, for other symbols see Figure 4.

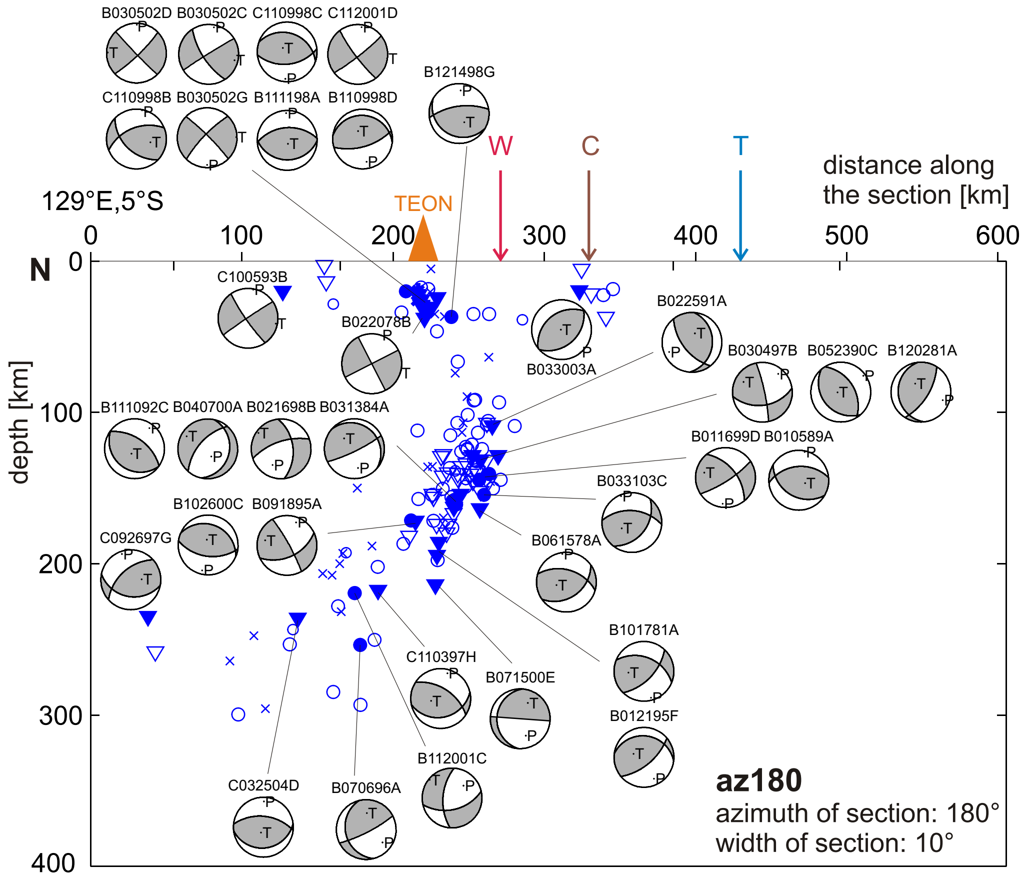

Figure 13. Vertical section az180. For the section position and symbols of earthquakes see Figure 3, for other symbols see Figure 4.

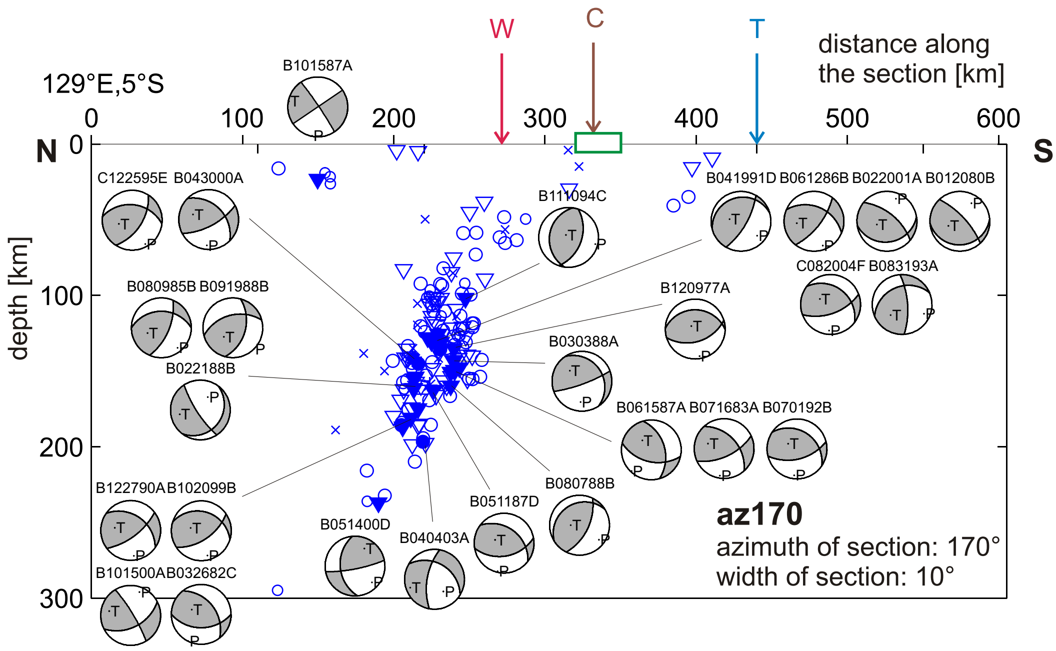

Figure 14. Vertical section az170. For the section position and symbols of earthquakes see Figure 3, for other symbols see Figure 4.

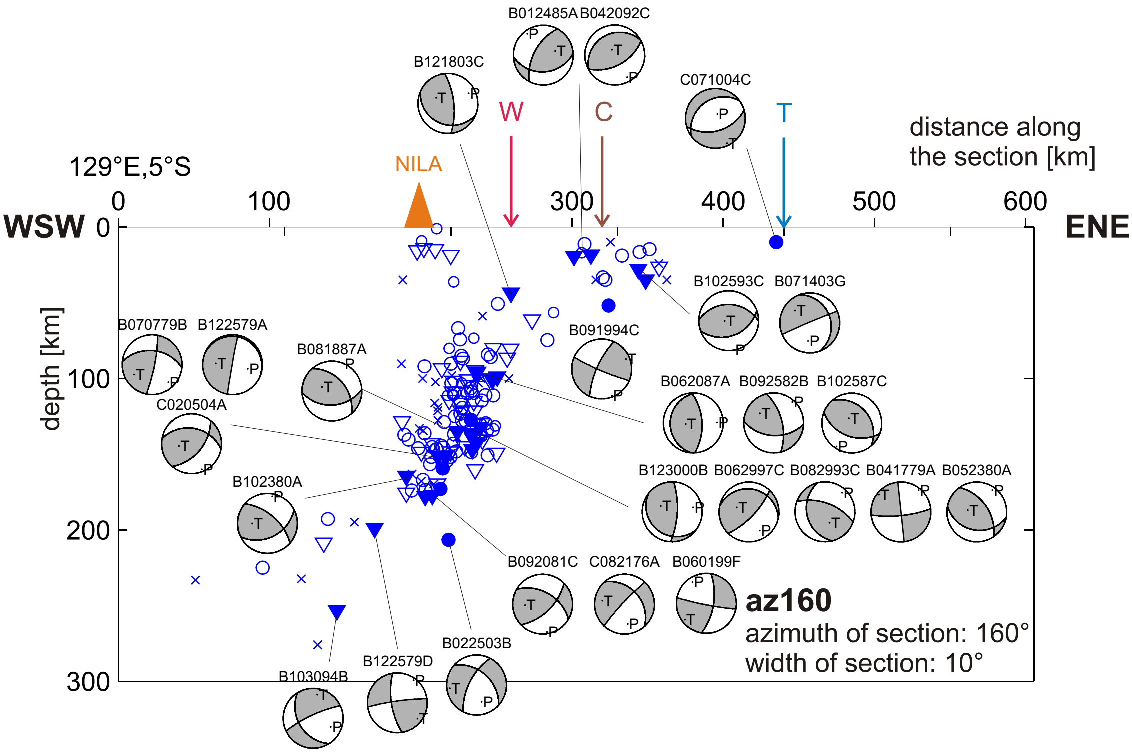

Figure 15. Vertical section az160. For the section position and symbols of earthquakes see Figure 3, for other symbols see Figure 4.

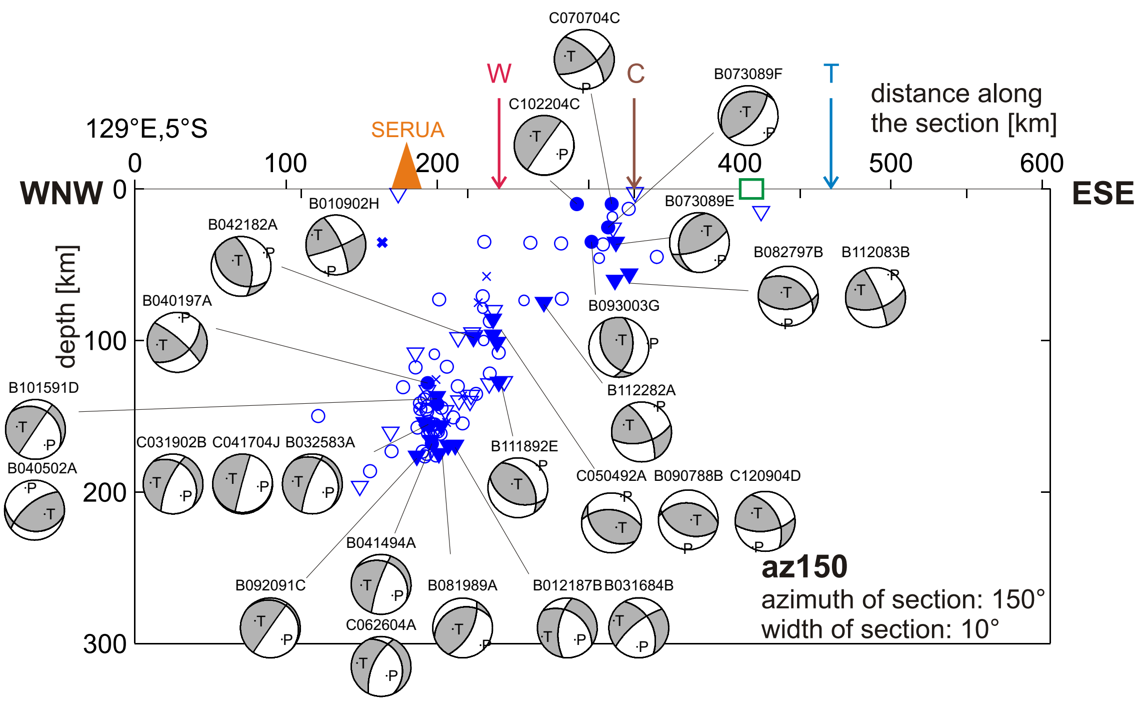

Figure 16. Vertical section az150. For the section position and symbols of earthquakes see Figure 3, for other symbols see Figure 4.

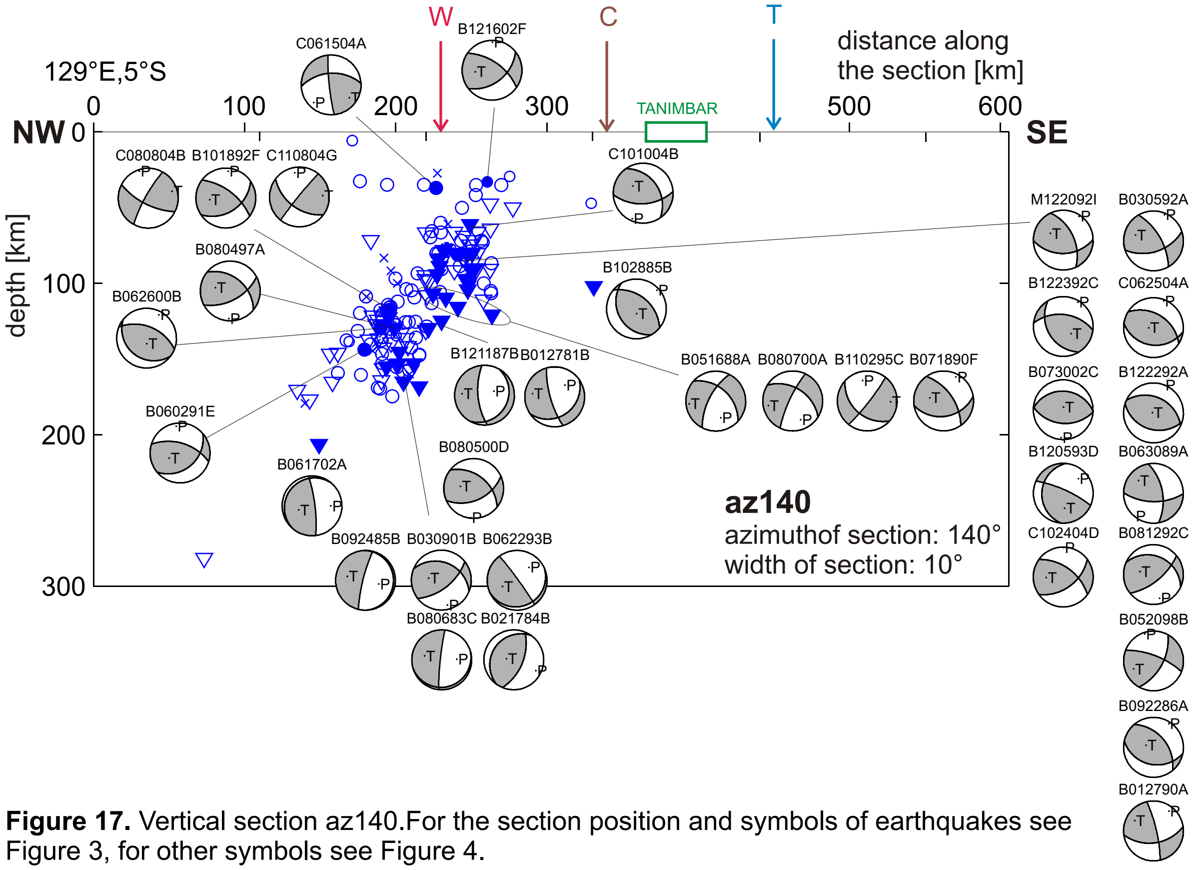

Figure 17. Vertical section az140.For the section position and symbols of earthquakes see Figure 3, for other symbols see Figure 4.

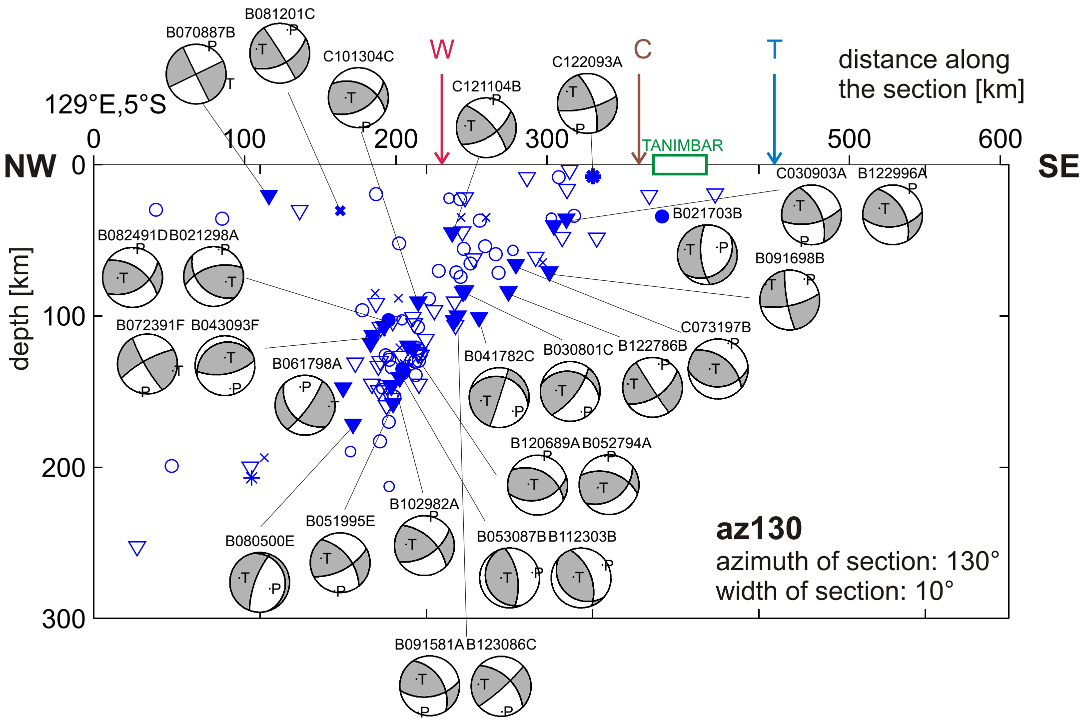

Figure 18. Vertical section az130.For the section position and symbols of earthquakes see Figure 3, for other symbols see Figure 4.

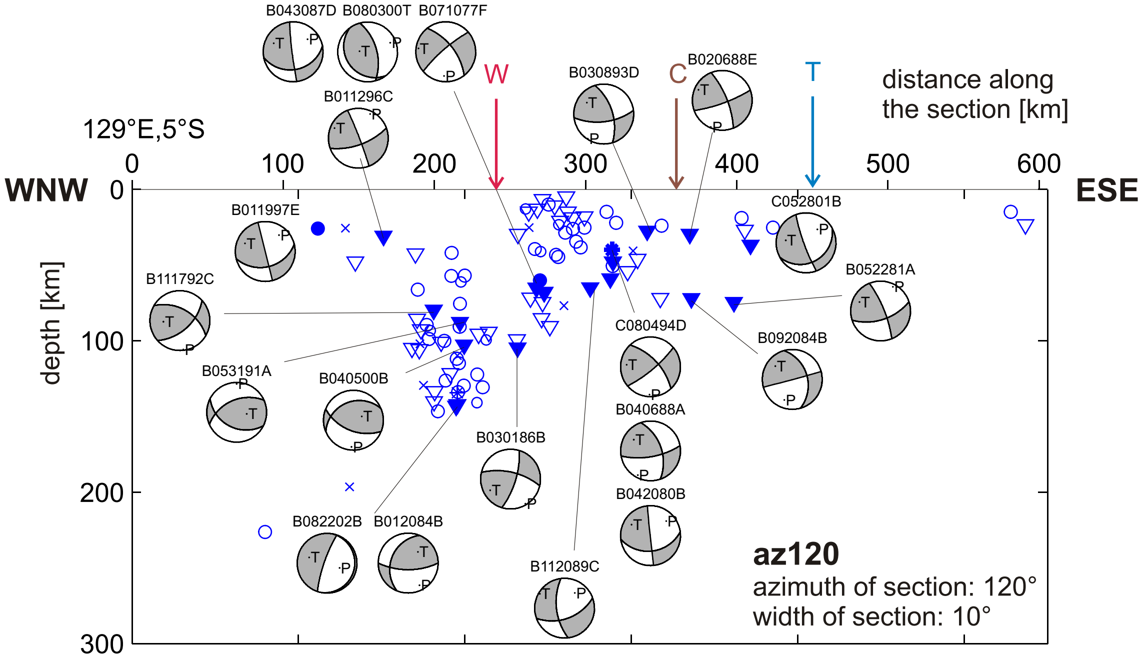

Figure 19. Vertical section az120. For the section position and symbols of earthquakes see Figure 3, for other symbols see Figure 4.

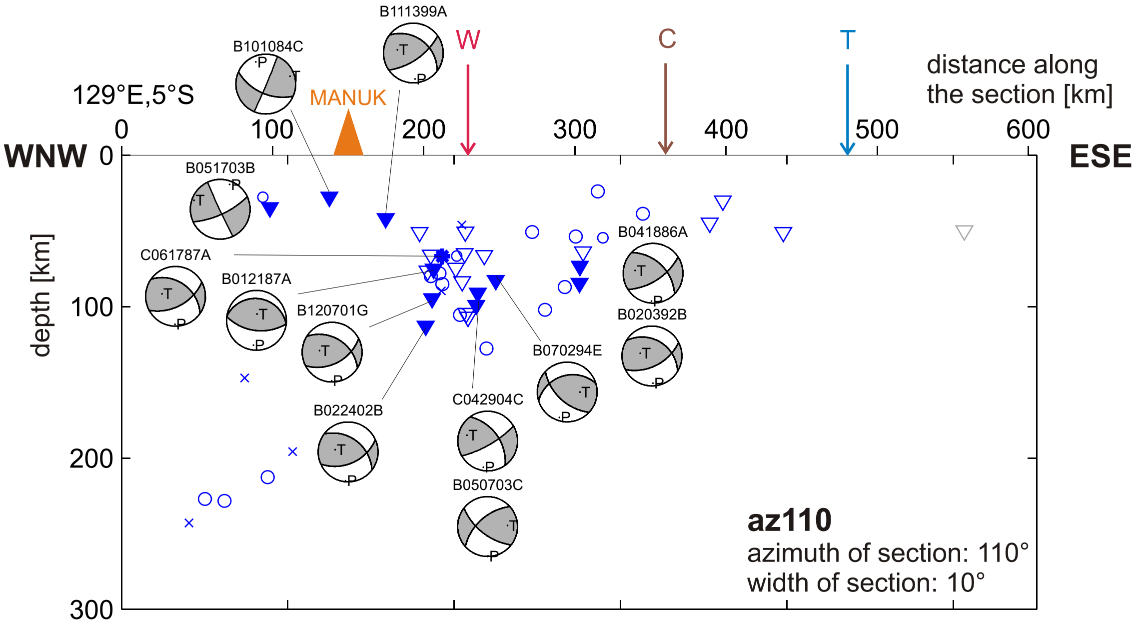

Figure 20. Vertical section az110. For the section position and symbols of earthquakes see Figure 3, for other symbols see Figure 4.

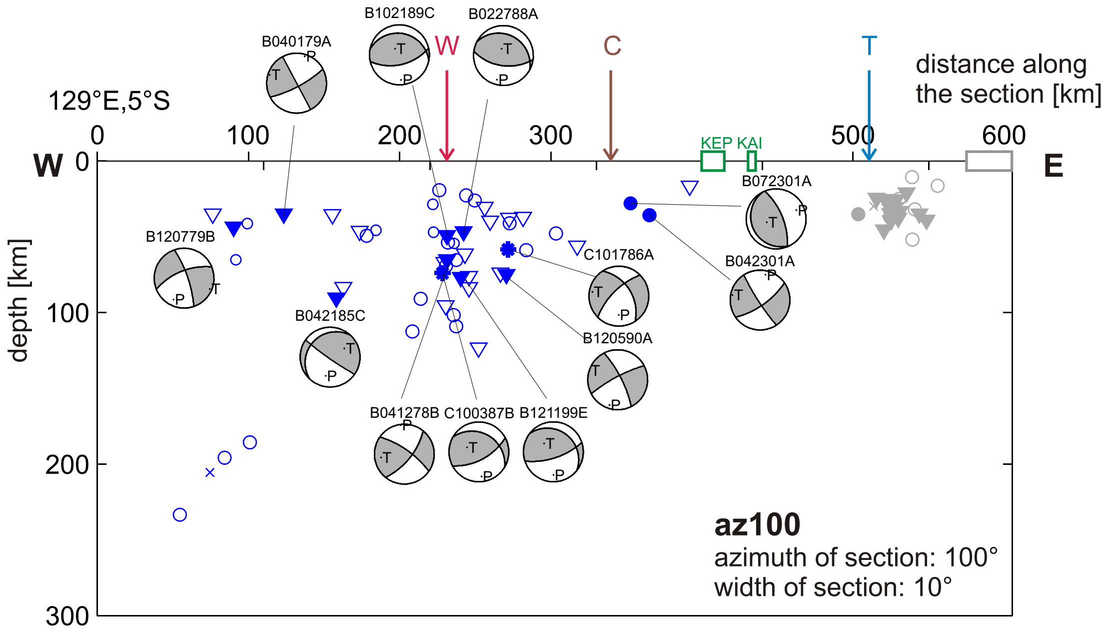

Figure 21. Vertical section az100. For the section position and symbols of earthquakes see Figure 3, for other symbols see Figure 4.

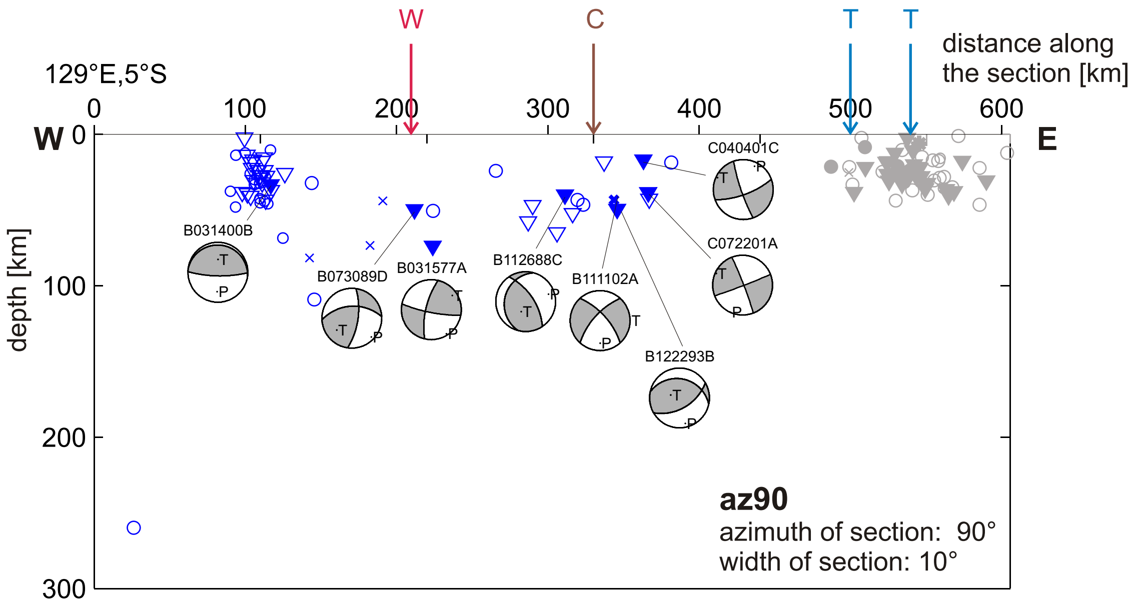

Figure 22. Vertical section az90. For the section position and symbols of earthquakes see Figure 3, for other symbols see Figure 4.

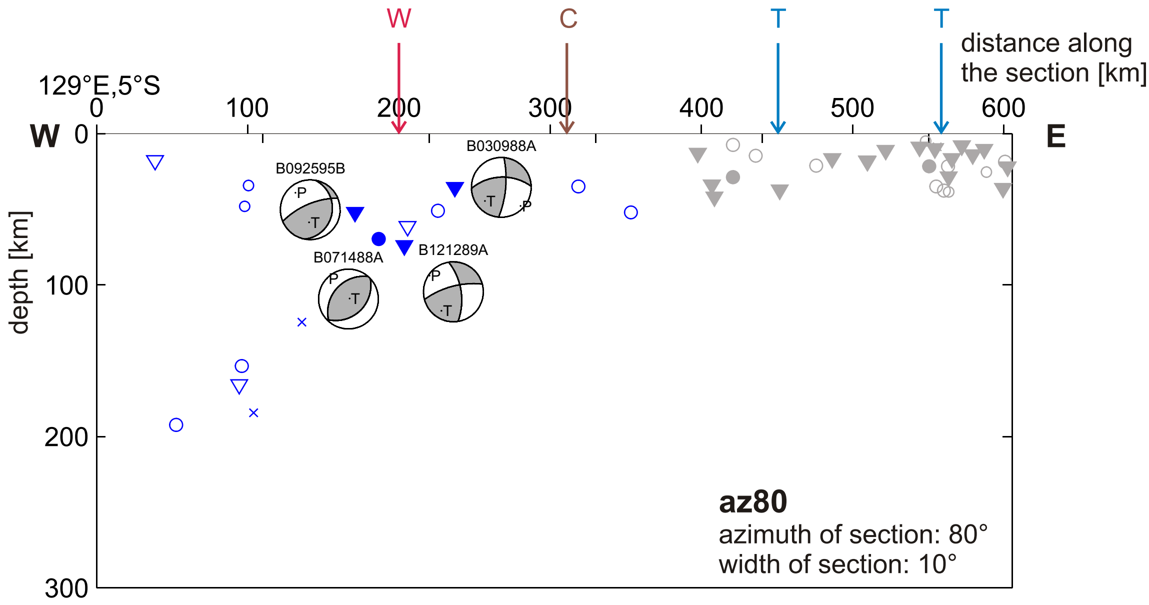

Figure 23. Vertical section az80. For the section position and symbols of earthquakes see Figure 3, for other symbols see Figure 4.

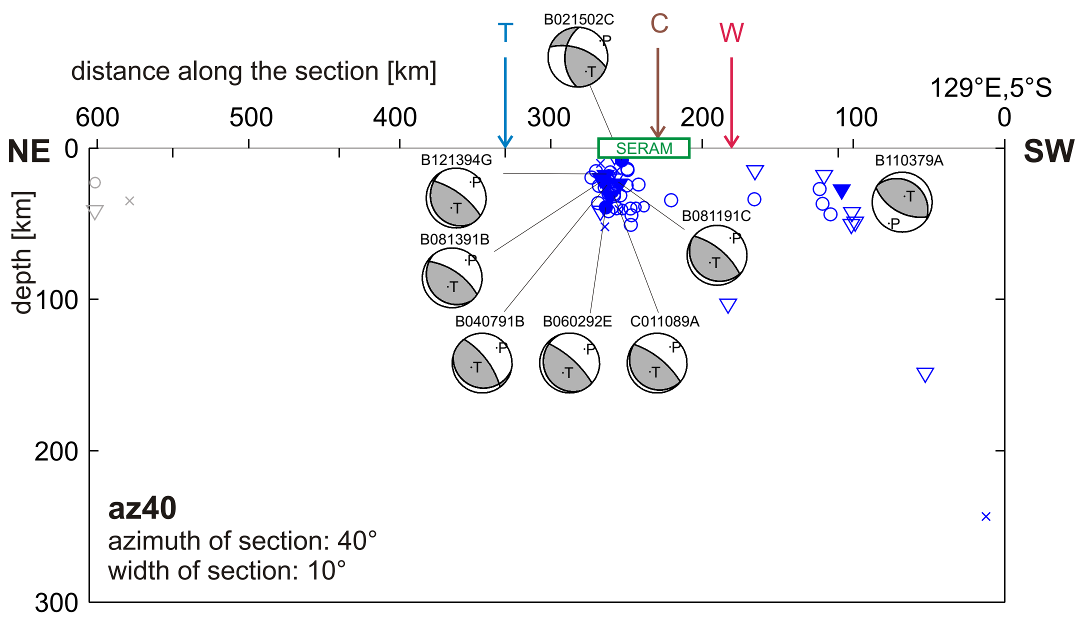

Figure 24. Vertical section az40. For the section position and symbols of earthquakes see Figure 3, for other symbols see Figure 4.

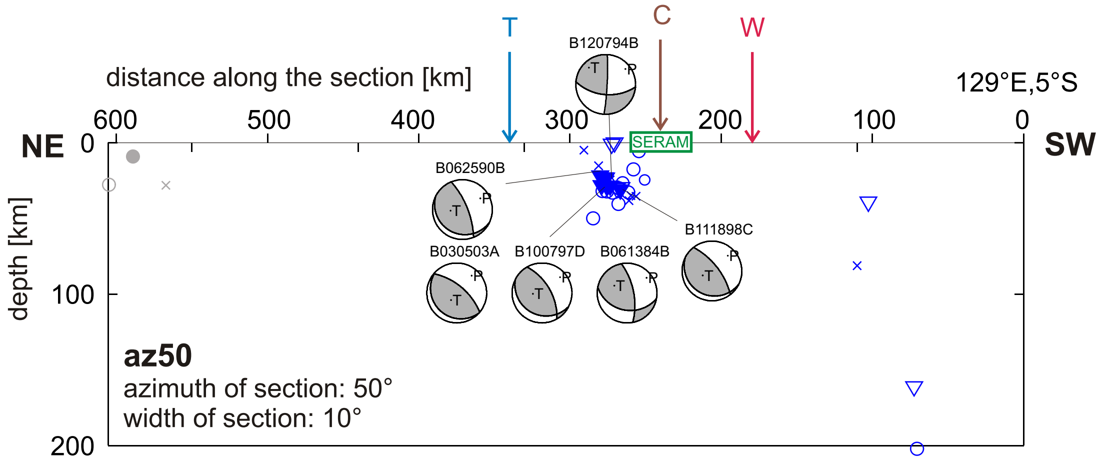

Figure 25. Vertical section az50. For the section position and symbols of earthquakes see Figure 3, for other symbols see Figure 4.

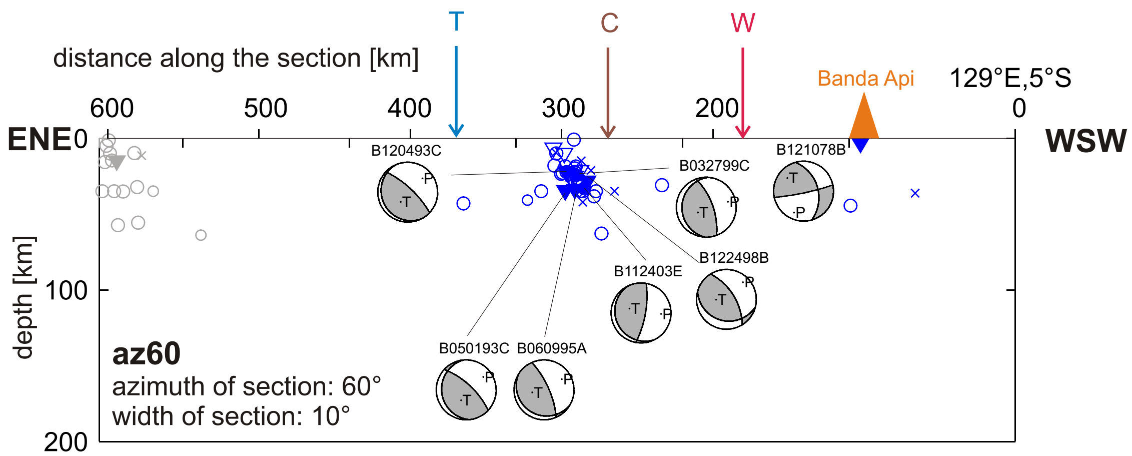

Figure 26. Vertical section az60. For the section position and symbols of earthquakes see Figure 3, for other symbols see Figure 4.

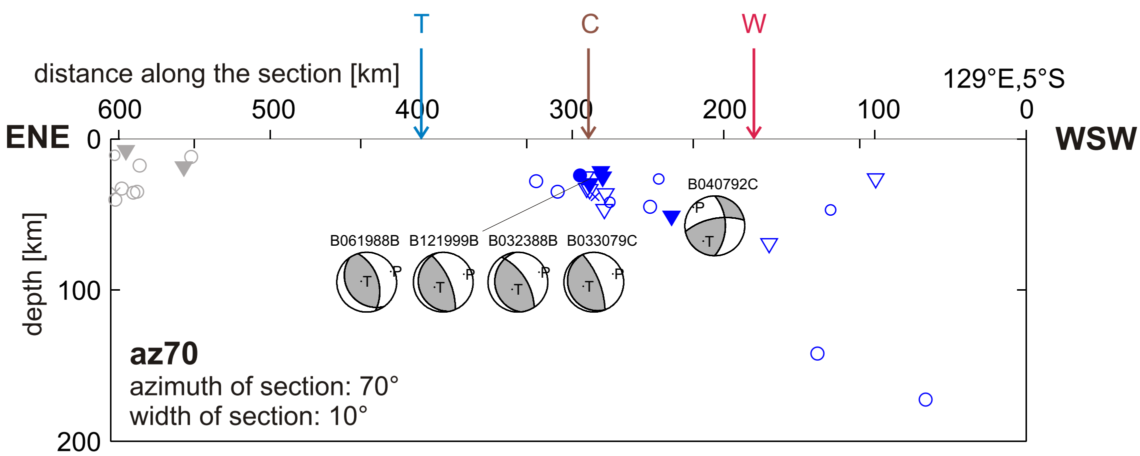

Figure 27. Vertical section az70. For the section position and symbols of earthquakes see Figure 3, for other symbols see Figure 4.

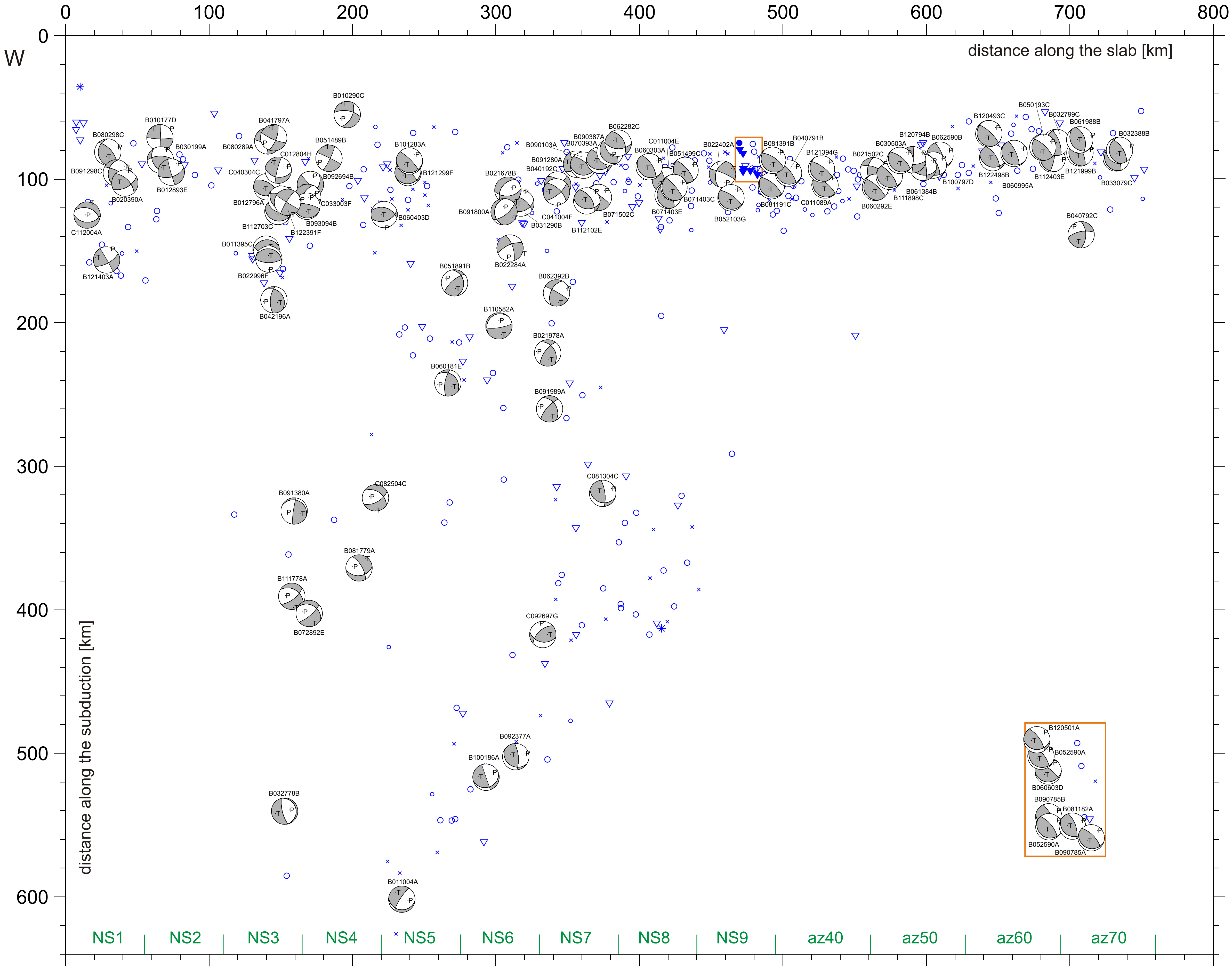

Figure 28. Longitudinal section along the Seram subduction. For the section position and symbols of earthquakes see Figure 3. Dip of the section is 50°. Triangular sections az40 - az70 are displayed as parallel strips indicated by green ticks. Focal mechanism diagrams are displayed in map view.

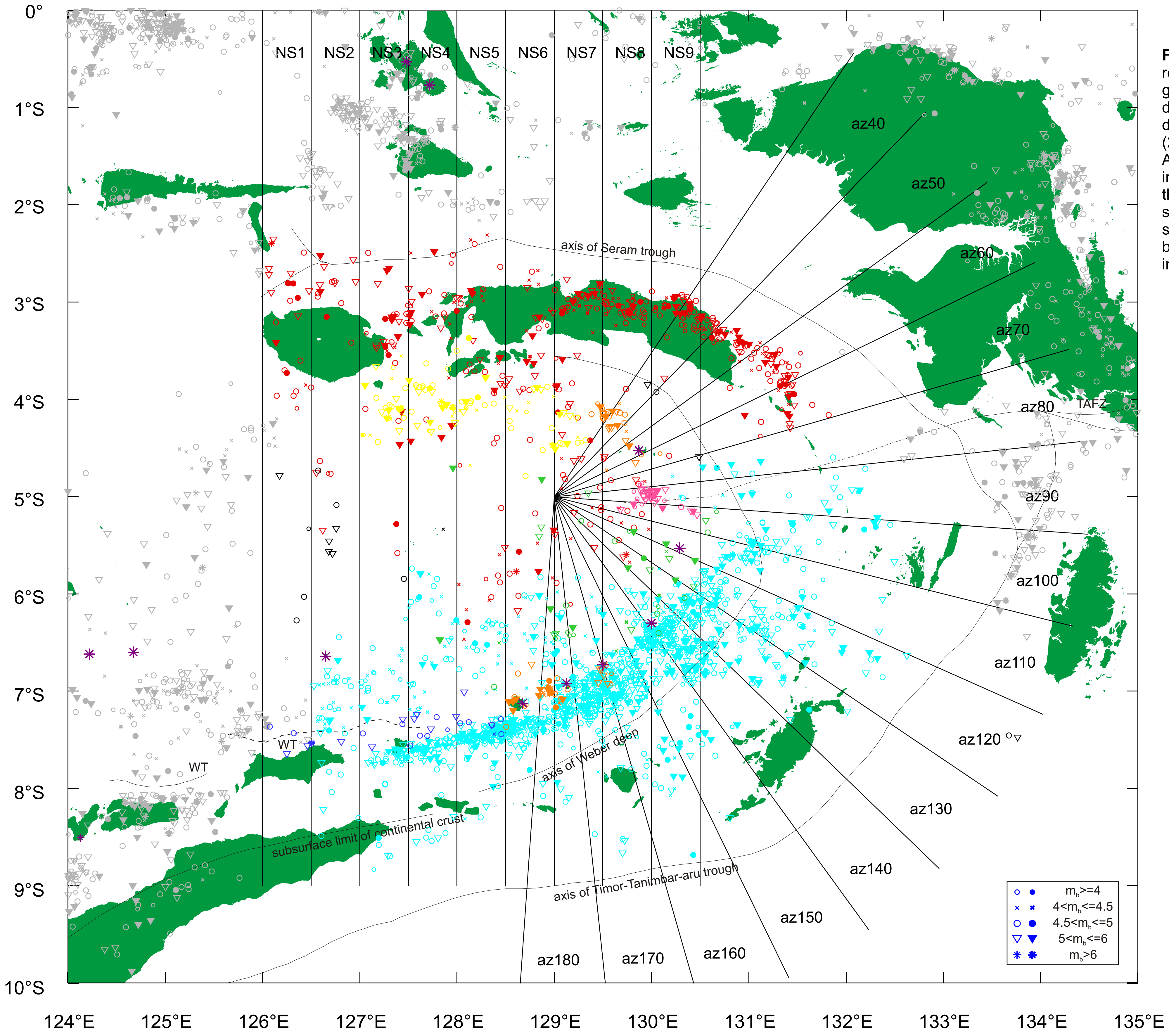

Figure 29. Intepreted epicentral map of the Banda Sea region. For the symbols of earthquakes see Figure 3. Main geomorphological elements of the Banda Sea region are denoted by black lines (Hamilton, 1978; see Figure 3), dashed line WT denotes Wetar thrust by Hinschberger et al. (2003), dashed line TAFZ denotes the continuation of Tarera-Aiduna fault zone inside the Banda Sea. Magenta asterisks indicate active volcanoes (see Figure 3), light blue symbols the southern WBZ, red symbols the northern WBZ, orange symbols SACs, pink symbols TAFZ, green and yellow symbols the overriding plate, grey symbols adjacet seismicity; black symbols indicate isolated events that were not interpreted (see text, Chapter 4).

5. Summary

1. The analysis of spatial distribution of global seismological data in the Banda Arc enabled to delimitate two Wadati-Benioff zones of two different subductions, which supports the two-slab idea of the arc. Sudden change in the trend of seismicity provides the strongest evidence for the two-slab model. Another evidence is the different depth of penetration of the slabs, different trend of seismic activity and different seismicity pattern within the WBZs. All these items are well demonstrated by the spatial distribution of earthquake foci. In sections NS3 - NS6 (Figures 6 - 9) two opposite dipping WBZs are clearly seen.

2. The trend of seismic activity, thickness and dip of the southern WBZ change abruptly along the southern limb of the arc. The WBZ is also unusually laterally bent. Shallow part of the WBZ is seismically less active than deeper parts. The most active and peculiar part of the WBZ of the southern subduction is the intermediate-depth, vertically situated domain. This is the unique feature of the Banda subduction which has been observed nowhere around the world. The distribution of earthquakes within the domain and the vertical orientation of the domain resemble a tear within the slab, but the nonuniform orientation of nodal planes of focal mechanisms does not confirm this interpretation.

3. The distribution of earthquakes within the northern WBZ is unique, too. Nowhere around the world, such an active vertical segment of shallow seismicity with uniform reverse focal mechanisms can be observed as in the Seram subduction. The available focal mechanisms in the segment point to reverse faulting. The intermediate-depth and deep part of the WBZ is seismically less active than the southern WBZ.

4. The collision of two opposite dipping slabs is an anomalous feature which can be observed only in the Banda Sea region. The collision is apparent in the area of the deepest penetration of the slabs in the depth of about 400 km.

5. High seismicity of the southern WBZ indicates that the subduction is still active in this part of the arc. On the other hand, the lack of seismicity beneath the Timor

island and shallow seismicity along the southern limb of the arc suggests that the subduction ceased there. The extinct volcanism north of Timor supports the recent cessation of subduction and an early stage of collision in the west part of the Banda arc (Vroon, 1992). The north-south convergence caused by northward movement of Australia is compensated in the back-arc region along the Wetar thrust (Hamilton, 1979; McCaffrey, 1989; Hinschberger et al., 2003, 2005). However, only 8 events along the Wetar thrust are no strong evidence that the Wetar thrust is the major tectonic structure of the southern part of the Banda Arc.

6. The earthquakes within the overriding plate are connected with volcanic activity or fault zones activity. Three seismically active columns (SAC) were delineated beneath the volcanoes Damar and Teon, Nila and Banda Api along the Banda volcanic arc. The volcanic activity and seismic activity below the volcanoes are induced by the process of subduction.

7. The extensive deformation of the Banda Basin has reverse and strike-slip focal mechanisms of earthquakes. Thrust earthquakes indicate that the Banda Basin is closing and strike-slip events reveal that the basin elongates in the west-eastern direction as it shortens in the north-south direction.

8. A plane approximation of the distribution of foci of the mainshock-aftershock sequences is an efficient tool searching for the parameters of respective planes representing the fracture zones. The distribution of earthquakes in one of the mainshock-aftershock sequences seems to be evidence that the Tarera-Aiduna fault continues inside the Banda Sea.

6. Conclusion

The goal of this thesis was to introduce me to seismology and tectonics, to familiarize me with seismological data and to show me how to use them for tectonic interpretations. The Banda Arc provides a good opportunity for its unique tectonic position and seismic activity. The Banda Arc is characterized by unusual surface morphology and curved shape, where two opposite dipping plates subduct and collide at the depth of their maximum penetration. The earthquake distribution within WBZs changes abruptly along the arc. The present-day tectonic setting of the Banda Arc is regarded as the only place in the world where the continent entered into the subduction process.

The method of analysis of earthquake distribution was shown to be an effective tool for investigating the process of subduction at convergent plate margins. Main results of this method summarize parameters that characterize the WBZs (see Chapter 4, page 31). However, the method does not enable a complete description due to the complexity of the Banda Arc.

The next work should be concentrated to usage of other methods (see Chapter 3.4, page 24) which can provide more detailed knowledge of individual structures mentioned in Chapter 5 (page 65).

Seismology is a powerful tool solving many geological and tectonic peculiarities; however it could not solve all of them, e.g. the debated origin and function of the Timor-Tanimbar-Aru troughs, the Seram trough and the Weber deep. A discussion with other geological and volcanological data would be necessary.

References

Audley-Charles, M.G. (1975): The Sumba fracture: a major discontinuity between eastern and western Indonesia. *Tectonophysics, 26,* 213-228.

Audley-Charles, M.G. (1981): Geometrical problems and implications of large scale overthrusting in the Banda Arc – Australian margin collision zone. From: *Thrust and Nappe Tectonics* (edited by K. R. McClay and N. J. Price) Special Publications of the Geological Society of London, 407-416.

Bird, P. (2003): An updated digital model of plate boundaries. *Geochemistry Geophysics Geosystems, 4(3)*, 1027, doi: 10.1029/2001GC000252.

Bock Y., Prawirodirdjo, L., Genrich, J.F., Stevens, C.W., McCaffrey, R., Subarya, C., Puntodewo, S.S. O. and Calais, E. (2003): Crustal motion in Indonesia from Global Positioning System measurements. *Journal of Geophysical Research*, *108*(B8), 2367, doi: 10.1029/2001JB000324.

Cardwell, R.K. and Isacks, B.L. (1978): Geometry of the Subducted Lithosphere Beneath the Banda Sea in Eastern Indonesia From Seismicity and Fault Plane Solutions. *Journal of Geophysical Research, 83*, 8B0127, 2825-2838.

Charlton, T.R. (1991): Postcollision extension in arc-continent collision zones, eastern Indonesia. *Geology, 19*, 28-31.

Čížková, H. (2005): Numerické simulace procesu litosférické subdukce. *Československý časopis pro fyziku, 2*, 135.

Daly, M.C., Hooper, B.G.D. and Smith, D.G. (1987): Terciary plate tectonics and basin evolution in Indonesia. Proceedings of the 16th Annual Convention Indonesian Petroleum Association 1987; 399-428.

Das, S. (2004): Seismicity gaps and the shape of the seismic zone in the Banda Sea region from relocated hypocenters. *Journal of Geophysical Research, 109*, B12303, doi: 10.1029/2004JB003192.

DeMets, Ch., Gordon, R.G., Argus, D.F. and Stein, S. (1994): Effect of recent revision to the geomagnetic reversal time scale on estimates of current plate motions. *Geophysical Research Letters, 21*, 20, 2191-2194.

Engdahl, E.R., van der Hilst, R. and Buland, R. (1998): Global Teleseismical Earthquake Relocation with Improved Travel Times and Procedures for Depth Determination. *Bulletin of the Seismological Society of America, 88*, 3, 722-743.

Fitch, T.J. (1970): Earthquake mechanisms and island arc tectonics in the Indonesian-Philippine region. *Bulletin of the Seismological Society of America, 60*, 2, 565-591.

Fitch, T.J. and Molnar, P. (1970): Focal Mechanisms along Inclined Earthquakes Zones in the Indonesia-Philippine Region. *Journal of Geophysical Research,* 75, 8, 1431-1444.

Hall, R. (1996): Reconstructing Cenozoic SE Asia. From: *Tectonic Evolution of Southeast Asia* (eds. R. Hall and D. J. Blundell), Geological Society Special Publication No. 106, 153-184.

Hall, R. and Blundell, D.J. (eds), 1996, *Tectonic Evolution of Southeast Asia*, Geological Society Special Publication No. 106.

Hall, R. (2002): Cenozoic geological and plate tectonic evolution of SE Asia and the SW Pacific: computer-based reconstructions, model and animations. *Journal of Asian Earth Sciences 20*, 353–431.

Hamilton, W. (1978): Tectonic map of the Indonesian region. *U.S. Geol. Survey.*

Hamilton, W. (1979): Tectonics of the Indonesian region. *U.S. Geol. Survey Professional Paper,1078*, 345pp, US Government Printing Office, Washington.

Hamilton, W.B. (2002): The Closed Upper-Mantle Circulation of Plate Tectonics. From: *Plate Boundary zones* (S. Stein and J. T. Freymueller), Geodynamic series, vol. 30.

Hanuš, V. and Vaněk, J. (1976): Intermediate aseismicity of the Andean subduction zone and recent andesitic volcanism. *Journal of Geophysics*, 42, 219-223.

Hanuš, V. and Vaněk, J. (1978): Tonga-Lau system: deep collision of subducted lithospheric plates. *Journal of Geophysics*, 44, 473-480.

Hanuš, V. and Vaněk, J. (1981): Plate tectonic interpretation of deep earthquakes between the Tonga-Lau and New Hebrides subduction zones. *Tectonosphysics*, *75*, T19-T28.

Hanuš, V. and Vaněk, J. (1985): Structure of Wadati-Benioff zones and volcanism produced by the process of subduction. *Tectonophysics, 112*, 51-67.

Hanuš, V. and Vaněk, J. (1991): Paleoplates buried in the upper mantle and the cyclic cvharacter of subduction. *Journal of Geodynamics*, *132*, 29-45.

Hanuš, V., Špičák, A. and Vaněk, J. (1996): Sumatran segment of the Indonesian subduction zone: morphology of the Wadati-Benioff zone and seismotectonic pattern of the continental wedge. *Journal of Southeast Asian Earth Sciences, 13*, no. 1, pp 39-60.

Hinschberger, F., Malod, J.A., Dyment, J., Honthaas, C., Réhault, J.-P. and Burhanuddin, S. (2001): Magnetic lineations constraints for the back-arc opening of the Late Neogene South Banda Basin (eastern Indonesia). *Tectonophysics*, 333, 47-59.

Hinschberger, F., Malod, J. A., Réhault, J.P. and Burhanuddin, S. (2003): Apport de la bathymétrie et de la géomorphologie a la géodynamique des mers de l'Est-indonésien. *Bulletin de la Société Géologique de France*, *174*, 6, 545-560.

Hinschberger, F., Malod, J.A., Réhault, J.-P., Villeneuve, M., Royer, J.-Y. and Burhanuddin, S. (2005): Late Cenozoic geodynamic evolution of eastern Indonesia. *Tectonophysics*, *404*, 91-118.

Isacks, B., Oliver, J. and Syker, L.R. (1968): Seismology and the New Global Tectonics. *Journal of Geophysical Research*, *73*, 5855-5899.

Jin, S. and Zhu, W. (2004): A revision of the parameters NNR-NUVEL-1A plate velocity model. *Journal of Geodynamics, 38*, 85-92.

Katili, J.A. (1975): Volcanism and Plate Tectonics in the Indonesian Island arcs. *Tectonophysics, 26*, 165-188.

Katili, J.A. (1989): Review of past and present geotectonic concepts of eastern Indonesia. *Netherlands Journal of Sea Research, 24 (2/3)*, 103-129.

McCaffrey, R., Molnar, P., Roecker, S.W. and Joyodiwiryo, Y.S. (1985): Microearthquake seismicity and fault plane solutions related to arc-continent collision in the eastern Sunda Arc, Indonesia. *Journal of Geophysical Research*, 90, B6, 4511-4528.

McCaffrey, R. (1988): Active Tectonics of the Eastern Sunda and Banda Arcs. *Journal of Geophysical Research, 93*, B12, 15163-15182.

McCaffrey, R. (1989): Seismological constrains and speculations on Banda arc tectonics. *Netherlands Journal of Sea Research, 24 (2/3)*, 141-152.

McCaffrey, R. (1996): Slip partitioning at convergent plate boundaries of SE Asia. From: *Tectonic Evolution of Southeast Asia* (eds R. Hall and D. J. Blundell), Geological Society Special Publication

No. 106, 3-18.

Metcalfe, I. (1996): Pre-Cretaceous evolution of SE Asian terranes. From: *Tectonic Evolution of Southeast Asia* (eds R. Hall and D. J. Blundell), Geological Society Special Publication No. 106, 97-122.

Milsom, J., Audley-Charles, M.G., Barber, A.J. and Carter, D.J. (1983): Geological-geophysical paradoxes of the Eastern Indonesian collision zone. From: *Geodynamics of the western Pacific-Indonesian region 11* (eds. T.W.C. Hilde and S. Uyeda), American Geophysical Union and Geological Society of America (1983), pp. 401–412 Geodynamics Series.

Milsom, J., Kaye S. and Sardjono (1996): Extension, collision and curvature in the eastern Banda arc. From: *Tectonic Evolution of Southeast Asia* (eds R. Hall and D. J. Blundell), Geological Society Special Publication No. 106, 85-94.

Milsom, J. (2001): Subduction in eastern Indonesia: how many slabs? *Tectonophysics, 338*, 167-178.

Packham, G. (1996): Cenozoic SE Asia reconstructions: reconstructing its aggregation and reorganization. From: *Tectonic Evolution of Southeast Asia* (eds R. Hall and D. J. Blundell), Geological Society Special Publication No. 106, 123-152.

Pairault, A.A., Hall, R. and Elders, Ch.F. (2003): Structural styles and tectonic evolution of the Seram Trough, Indonesia. *Marine and Petroleum Geology*, 20, 10, 1141-1160, doi: 10.1016/j.marpetgeo. 2003.10.001.

Papp, Z. (1980): A three-dimensional model of the seismicity in the Banda Sea region, *Tectonophysics*, 69, 63-83.

Puntodewo, S.S.O., McCaffrey, R., Calais, E., Bock, Y., Rais, J., Subarya, C., Poewariardi, R., Stevens, C., Genrich, J., Fauzi, Zwick, P. and Wdowinski, S. (1994): GPS measurements of crustal deformation within the Pacific-Australia plate boundary zone in Irian Jaya, Indonesia. *Tectonophysics,* 273, 141-153.

Pustito, N. T. and Shimazaki, K. (1995): Mantle structure and seismotectonic of the Sunda and Banda Arcs. *Tectonophysics*, *251*, 215-228.

Ritsema, A.R., Sudarmo, R.P. and Putu Pudja, I. (1989): The generation of the Banda Arc on the basis of its seismicity. *Netherlands Journal of Sea Research, 24 (2/3)*, 165-172.

Richardson, A.N. and Blundell, D.J. (1996): Continental collision in the Banda arc. From: *Tectonic Evolution of Southeast Asia* (eds R. Hall and D. J. Blundell), Geological Society Special Publication No. 106, pp. 47-60.

Schöffel, H.-J. and Das, S. (1999): Fine details of the Wadati-Benioff zone under Indonesia and its geodynamic implications, *Journal of Geophysical Research, 104*, B6, 13101-13114.

Simandjuntak, T.O. and Barber, A.J. (1996): Constrasting tectonic styles in the Neogene orogenic belts of Indonesia. From: *Tectonic Evolution of Southeast Asia* (eds R. Hall and D.J. Blundell), Geological Society Special Publication No. 106.

Simkin, T., Siebert, L., McClelland, L., Bridge, D., Newhall, Ch. and Latter, J.H. (1981): Volcanoes of the World. Smithsonian Institute, Hutchinson Ross, Stoudsburg Pa.

Slancová, A., Špičák, A., Hanuš, V. and Vaněk, J. (2000): How the state of stress varies in the Wadati-Benioff zone: indications from focal mechanisms in the Wadati-Benioff zone beneath Sumatra and Java. *Geophysical Journal International*, *143*, 909-930.

Snyder, D.B., Milsom, J. and Prasetyo, H. (1996a): Geophysical evidence for local indentor tectonics in the Banda arc east of Timor. From: *Tectonic Evolution of Southeast Asia* (eds R. Hall and D.J. Blundell), Geological Society Special Publication No. 106, 153-184.

Snyder, D.B., Prasetyo, H., Blundell, D.J., Pigram, C.J., Barber, A.J., Richardson, A. and Tjokosaproetro, S. (1996b): A dual doubly vergent orogen in the Banda Arc continent-arc collision zone as observed on deep seismic reflection profiles. *Tectonics, 15*, 1, 34-53.

Špičák, A., Hanuš, V. and Vaněk, J. (2002): Seismic activity around and under Krakatau volcano, Sunda Arc: constraints to the source region of island arc volcanism. *Studia Geophysica et Geodaetica*, *46*, 545-565.

Špičák, A., Hanuš, V. and Vaněk, J. (2004): Seismicity pattern: an indicator of source region of volcanism at convergent plate margins. *Physics of the Earth and Planetary Ineriors*, 141, 303-326.

Špičák, A., Hanuš, V. and Vaněk, J. (2005): Seismotectonic pattern and the source region of volcanism in the central part of Sunda arc. *Journal of Southeast Asian Earth Sciences,* 25, 583-600.

Špičák,A., Hanuš, V. and Vaňek, J. (2007a): Earthquake occurance along the Java trench in front of the onset of the Wadati-Benioff zone: Beginning of a new subduction cycle? *Tectonics, 26*, TC1005, doi: 10.1029/2005TC001867.

Špičák, A., Hanuš, V., Vaněk, J. and M. Běhounková (2007b): Internal tectonic structure of the Central American Wadati-Benioff zone based on analysis of aftershock sequences. *Journaql of Geophysical Research*, *112*, B09304, doi: 10.1029/2006JB004318.

Tandon, K., Lorenzo, J.M., Widiyantoro, S. and O'Brien, G.W. (2002): Variations in Inelastic Failure of Subducting Continental Lithosphere and Tectonic Dwevelopement: Australia-Banda Arc Convergence. From: *Plate Boundary zones* (eds S. Stein J. T. Freymueller), Geodynamic series, vol. 30.

Vaněk, J., Hanuš, V., Christova, C. and Simeonova, S. (1987): Morphology of the Wadati-Benioff zone in the Helenic arc. *Journal of Geodynamics, 8*, 79-83.

Vaněk, J. and Hanuš, V. (1988): Historical disastrous earthquakes and deep fracture zones in Ecuador. Historical Seismograms and Earthquakes of the World (eds. W.H.K. Lee, H. Meyers, K. Shimazaki), Academic Press, San Diego, 362-369.

Vaněk, J. and Hanuš, V. (1990): Seismicity and deep structure of the Indo-Burman plate margin, *Journal of Southeast Asian Earth Sciences, 4*, 2, 147-157.

Vaněk, J., Špičák, A. and Hanuš, V. (2000): Position of the disastours 1999 Puebla earthquake in the seismotectonic pattern of Mexico. *Bulletin of the Seismological Society of America*, 90, 786-789.

Venzke, E., Wunderman, R. W., McClelland, L., Simkin, T., Luhr, J. F., Siebert, L. and Mayberry, G. (2002): Global Volcanism, 1968 to the Present. *Smithsonian Institution, Global Volcanism Program Digital Information Series*, GVP-4 (http://www.volcano.si.edu/reports/).

Vroon, P.Z. (1992): Subduction of continental material in the Banda arc, Eastern Indonesia: Sr-Nd-Pb isotope and trace-element evidence from volcanics and sediments. *Fac Aardwetenschappen der Rijksuniversiteit te Utrecht,* 205 p.

Widiyantoro, S. and van der Hilst, R. (1996): Structure and Evolution of Lithospheric Slab beneath the Sunda Arc, Indonesia. *Science, 271*, 1566-1570.

Widiyantoro, S. and van der Hilst, R. (1997): Mantle structure beneath Indonesia inferred from high-resolution tomographic imaging. *Geophysical Journal International, 130*, 167-182.

Willemann, R.J. and Storchak, D.A. (2001): Data Collection at the International seismological centre, http://www.isc.ac.uk/doc/analysis/2001p1/index.html.